

Supporting Information

Circularly polarized phosphorescence with large dissymmetry factor from a helical platinum(II) complex

Masahiro Ikeshita,^{‡*}a Shinya Watanabe,^{‡*}a Seika Suzuki,^b Shota Tanaka,^c Shingo Hattori,^c Kazuteru Shinozaki,^c Yoshitane Imai^{*b} and Takashi Tsuno^{*a}

^a Department of Applied Molecular Chemistry, College of Industrial Technology, Nihon University, Narashino, Chiba 275-8575, Japan

^b Department of Applied Chemistry, Faculty of Science and Engineering, Kindai University, 3-4-1 Kowakae, Higashi-Osaka, Osaka 577-8502, Japan

^c Graduate School of Nanobioscience, Yokohama City University 22-2 Seto, Kanazawa-ku, Yokohama 236-0027, Japan

[‡] M. I. and S. W. contributed equally to this work

Table of Contents

- 1. Instrumentation and Materials**
- 2. Synthetic Procedures and Characterization**
- 3. Single Crystal X-ray Diffraction Analysis**
- 4. NMR Analysis**
- 5. Photophysical Properties**
- 6. Computational Details**
- 7. Cartesian Coordinates (in Å)**
- 8. References**

1. Instrumentation and Materials

Instruments

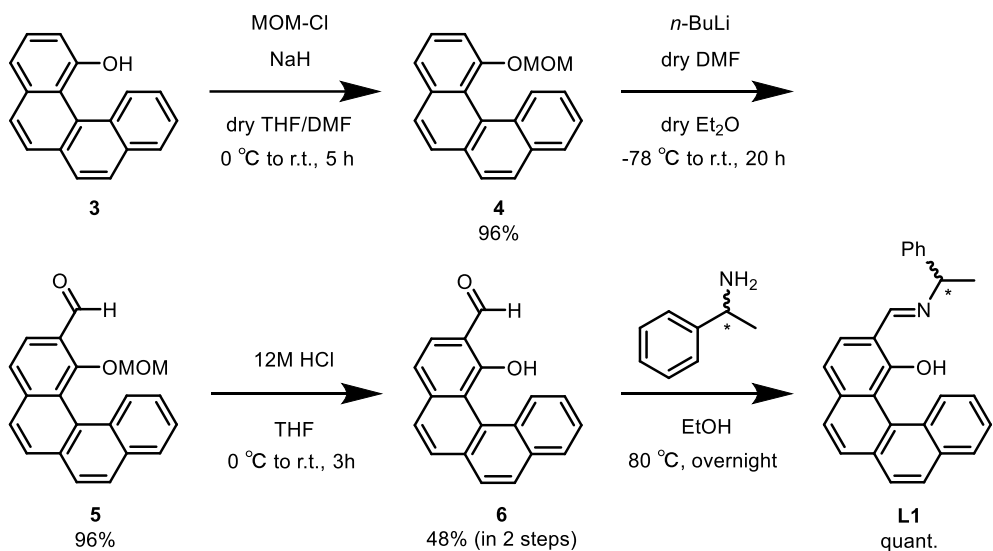
Melting points were measured by a ATM-01 melting temperature measurement device (AS ONE Corporation). IR spectra were acquired with a JASCO FT/IR4100ST spectrometer. High-resolution mass spectrometry was recorded on Bruker micrOTOF II spectrometer. ¹H and ¹³C NMR spectra were recorded on Bruker Avance III 500 spectrometers, TMS as internal standard. Elemental analyses were performed on a YANAKO MT-5 at A-Rabbit-Science Japan Co., Ltd. UV-vis absorption spectra were obtained on a SHIMADZU UV-1900i spectrophotometer. CD spectra were recorded on a Jasco J-720 spectropolarimeter. Emission spectra were obtained on a FP-6500 spectrometer. Emission lifetimes were determined through single-exponential curve-fitting of emission intensity data recorded over time with a Tektronix TDS320 digital oscilloscope after pulsed excitation at 355 nm using a Continuum Surelite Nd:YAG laser. CPL spectra were obtained at room temperature using a JASCO CPL-300 spectrofluoropolarimeter. Optical rotation was measured on a Jasco DIP-370 digital polarimeter.

Materials

(*R*)- and (*S*)-1-phenylethylamine (Kanto Chemical), potassium *tert*-butoxide (Kanto Chemical), potassium tetrachloroplatinate(II) (Kanto Chemical), 1-phenylisoquinoline (TCI), sodium hydride (dispersion in paraffin liquid) (Kanto Chemical), chloromethyl methyl ether (TCI), *n*-butyllithium (in *n*-hexane, *ca.* 1.6 mol/L) (Kanto Chemical), 2-ethoxyethanol (Fujifilm Wako), dry tetrahydrofuran (Kanto Chemical), dry *N,N*-dimethylformamide (Kanto Chemical), dry toluene (Kanto Chemical) and dry dimethyl sulfoxide (Kanto Chemical) were obtained from commercial sources and were used without further purification. Benzo[*c*]phenanthren-1-ol (**3**)^{S1}, Di- μ -chlorobis[2-(1-isoquinolinyl- κ N)phenyl- κ C]diplatinum ([Pt(piq)(μ -Cl)]₂)^{S2} and 2-[[[(1*R* or 1*S*)-1-phenylethyl]imino]methyl]phenol (**L2**)^{S3} were prepared according to the literature procedure.

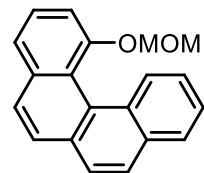
2. Synthetic Procedures and Characterization

Preparation of L1



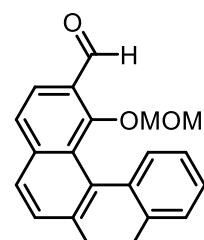
1-(Methoxymethoxy)benzo[c]phenanthrene (4)

A solution of benzo[c]phenanthren-1-ol (**3**)^{S1} (186 mg, 0.829 mmol, 1.00 equiv.) in dry THF (5 mL) was added to a suspension of sodium hydride (60% suspension in mineral oil, 39.8 mg, 0.995 mmol, 1.20 equiv.) in dry THF/DMF (5/2 mL) under nitrogen atmosphere at 0 °C. After stirring for 1 h, chloromethyl methyl ether (100 mg, 1.24 mmol, 1.50 equiv.) was added, and the reaction was then stirred for overnight at room temperature. The reaction mixture was quenched with water and then extracted with EtOAc (20 mL x 3). The organic layers were dried over anhydrous MgSO₄. After the removal of the solvent, the crude product was purified by column chromatography (SiO₂, *n*-hexane/EtOAc 100:0 to 4:1) to afford 1-(methoxymethoxy)benzo[c]phenanthrene (**4**) as a brown solid (183 mg, 77% yield).
 m.p. 168 °C (decomp); IR (KBr): 1157 cm⁻¹ (C-O); ¹H NMR (CDCl₃, 500 MHz) δ = 8.32 (d, *J* = 8.2 Hz, 1H), 7.97–7.91 (m, 2H), 7.86–7.79 (m, 2H), 7.77 (d, *J* = 7.80 Hz, 1H), 7.70 (dd, *J* = 7.78, 1.07 Hz, 1H), 7.60 (t, *J* = 7.93 Hz, 1H), 7.57–7.46 (m, 3H), 4.93 (s, 2H), 3.37 ppm (s, 3H); ¹³C NMR (CDCl₃, 125 MHz) δ = 155.0, 135.2, 132.4, 131.2, 131.3, 130.1, 127.7, 127.2, 126.94, 126.85, 126.7, 125.9, 125.8, 125.5, 123.6, 122.2, 121.0, 112.8, 96.1, 56.6 ppm; HRMS (APCI+): m/z [M+H]⁺ calcd for C₂₀H₁₇O₂: 289.1223; found: 289.1237.



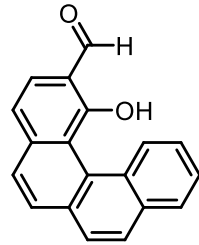
1-Methoxymethoxy[c]phenanthrene-2-carbaldehyde (5)

n-BuLi (in *n*-hexane, *ca.* 1.60 mol/L, 13.1 mL, 20.9 mmol, 3.00 equiv.) was slowly added to a solution of **4** (2.01 g, 6.97 mmol, 1.00 equiv.) in dry Et₂O (110 mL) at -78 °C under a nitrogen atmosphere. The mixture was stirred for 2 h at room temperature. After cooling to 0 °C, dry DMF (2.16 mL, 27.9 mmol, 4.00 equiv.) was added dropwise. The solution was allowed to warm to room temperature and stirred for overnight. The reaction was quenched with a saturated NH₄Cl solution and was extracted with EtOAc (40 mL x 3). The organic layers were dried over anhydrous MgSO₄. After removal of the solvent, the crude 1-(methoxymethoxy)benzo[c]phenanthrene-2-carbaldehyde (**5**) was obtained, which used directly in the next step without further purification.



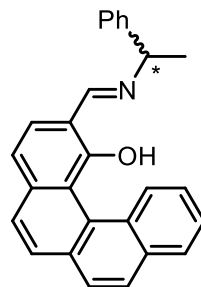
1-Hydroxybenzo[*c*]phenanthrene-2-carbaldehyde (**6**)

To a solution of **5** in THF (120 mL) at 0 °C was added to 12 M HCl (30 mL) slowly. The mixture was stirred at room temperature for 3 h. After that, the mixture was poured into water, and was extracted with EtOAc (40 mL x 3), followed by drying over anhydrous MgSO₄. After the removal of the solvent, the crude product was purified by column chromatography (SiO₂, *n*-hexane/EtOAc 4:1). Crystallization from CH₂Cl₂/*n*-hexane gave 1-hydroxybenzo[*c*]-phenanthrene-2-carbaldehyde (**6**) as a yellow solid in 48% yield (0.914 g, overall yield over two reaction steps). m.p. 165–170 °C; IR (KBr): 3343 cm⁻¹ (OH), 1743 cm⁻¹ (C=O); ¹H NMR (CDCl₃, 500 MHz) δ = 13.05 (s, 1H), 10.09 (s, 1H), 8.36 (dd, *J* = 8.2, 0.6 Hz, 1H), 8.00–7.90 (m, 3H), 7.80 (d, *J* = 6.4 Hz, 1H), 7.79 (d, *J* = 6.1 Hz, 1H), 7.71 (d, *J* = 8.2 Hz, 1H), 7.63–7.53 ppm (m, 3H); ¹³C NMR (CDCl₃, 125 MHz) δ = 196.6, 161.8, 139.4, 133.1, 131.9, 131.5, 131.4, 129.5, 128.8, 128.7, 121.6, 127.3, 126.7, 126.4, 125.6, 124.2, 119.7, 119.5, 115.9 ppm; HRMS (APCI+): m/z [M+H]⁺ calcd for C₁₉H₁₃O₂: 273.0910; found: 273.0929.



2-[[[(1*R* or 1*S*)-1-phenylethyl]imino]methyl]benzo[*c*]phenanthren-1-ol (**L1**)

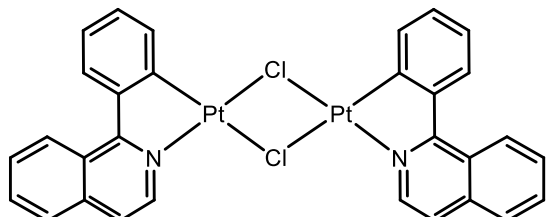
A mixture of (*R*) or (*S*)-1-phenylethylamine (43.8 mg, 0.361 mmol, 1.20 equiv.) and **6** (82.0 mg, 0.301 mmol, 1.00 equiv.) in EtOH (10 mL) was refluxed for overnight. Crystallization from EtOH gave 2-[[[(1*R* or 1*S*)-1-phenylethyl]imino]methyl]benzo[*c*]phenanthren-1-ol (**L1**) as an orange solid (113 mg, quant.).



m.p. 80–99 °C; IR (KBr): 3390 cm⁻¹ (OH), 1612 cm⁻¹ (C=N); ¹H NMR (CDCl₃, 500 MHz) δ = 14.84 (br s, 1H), 8.49 (d, *J* = 8.5 Hz, 1H), 8.27 (d, *J* = 5.8 Hz, 1H), 7.91 (dd, *J* = 7.9, 1.2 Hz, 1H), 7.89 (d, *J* = 8.5 Hz, 1H), 7.82 (d, *J* = 8.5 Hz, 1H), 7.76 (d, *J* = 8.5 Hz, 1H), 7.69 (d, *J* = 8.5 Hz, 1H), 7.56 (ddd, *J* = 8.0, 6.9, 1.2 Hz, 1H), 7.49 (ddd, *J* = 8.4, 6.9, 1.5 Hz, 1H), 7.40–7.34 (m, 4H), 7.32–7.27 (m, 2H), 7.19 (d, *J* = 8.5 Hz, 1H), 4.73 (q, *J* = 6.7 Hz, 1H), 1.72 ppm (d, *J* = 6.7 Hz, 3H); ¹³C NMR (CDCl₃, 125 MHz) δ = 169.2, 162.0, 142.9, 138.1, 133.0, 131.9, 131.6, 129.9, 129.6, 128.9 (2C), 128.8, 128.5, 127.7, 127.2, 126.8, 126.4, 126.0, 125.8, 123.5, 122.7, 116.5, 112.5, 64.3, 24.2 ppm; HRMS (APCI+): m/z [M+H]⁺ calcd for C₂₇H₂₂NO: 376.1696; found: 376.1719; (*S*)-**5**: [α]_D²⁵ = +124 (c 0.001, CHCl₃), (*R*)-**5**: [α]_D²⁵ = -122 (c 0.001, CHCl₃).

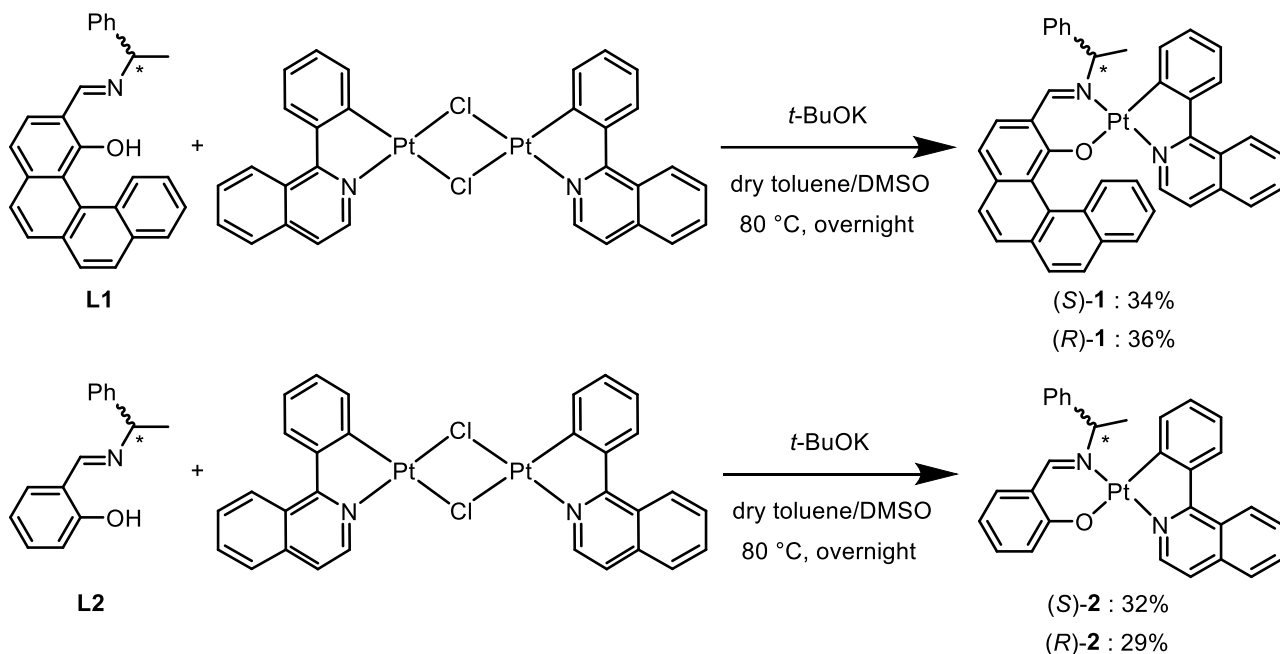
Di- μ -chlorobis[2-(1-isoquinolinyl- κ N)phenyl- κ C]diplatinum ([Pt(piq)(μ -Cl)]₂)^{S2}

A mixture of K₂PtCl₄ (500 mg, 1.00 mmol, 1.00 equiv.) and 1-phenylisoquinoline (246 mg, 1.20 mmol, 1.20 equiv.) in 2-ethoxyethanol/H₂O (15/5 mL) was warmed at 80 °C for 16 h. After cooling down to room temperature, the mixture was precipitated after the addition of H₂O (30 mL), filtered, and washed with H₂O (20 mL) and EtOH (20 mL). After drying under reduced pressure, di- μ -chlorobis[2-(1-isoquinolinyl- κ N)phenyl- κ C]diplatinum ([Pt(piq)(μ -Cl)]₂) was obtained as a dark green solid (391 mg, 45% yield).



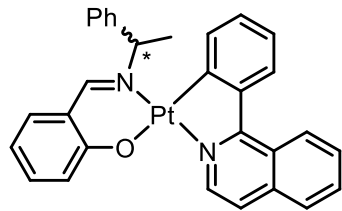
General procedure for platinum complexes

A solution of corresponding chiral ligands **L1** or **L2** (2.00 equiv.), $[\text{Pt}(\text{piq})(\mu\text{-Cl})_2$ (1.00 equiv.), potassium *tert*-butoxide (2.50 equiv.) in dry toluene/DMSO (8/2 mL) was warmed at 80 °C for overnight. After that, the mixture was poured into water, and was extracted with EtOAc (20 mL x 3), followed by drying over anhydrous MgSO_4 . After the removal of the solvent, the residue was separated by column chromatography (SiO_2 , eluent; CH_2Cl_2). The purification by gel permeation chromatography using a recycling preparative HPLC system (eluent as CHCl_3) gave (*S*)-**1** (34%), (*R*)-**1** (36%), (*S*)-**2** (32%) and (*R*)-**2** (29%) as red solids.

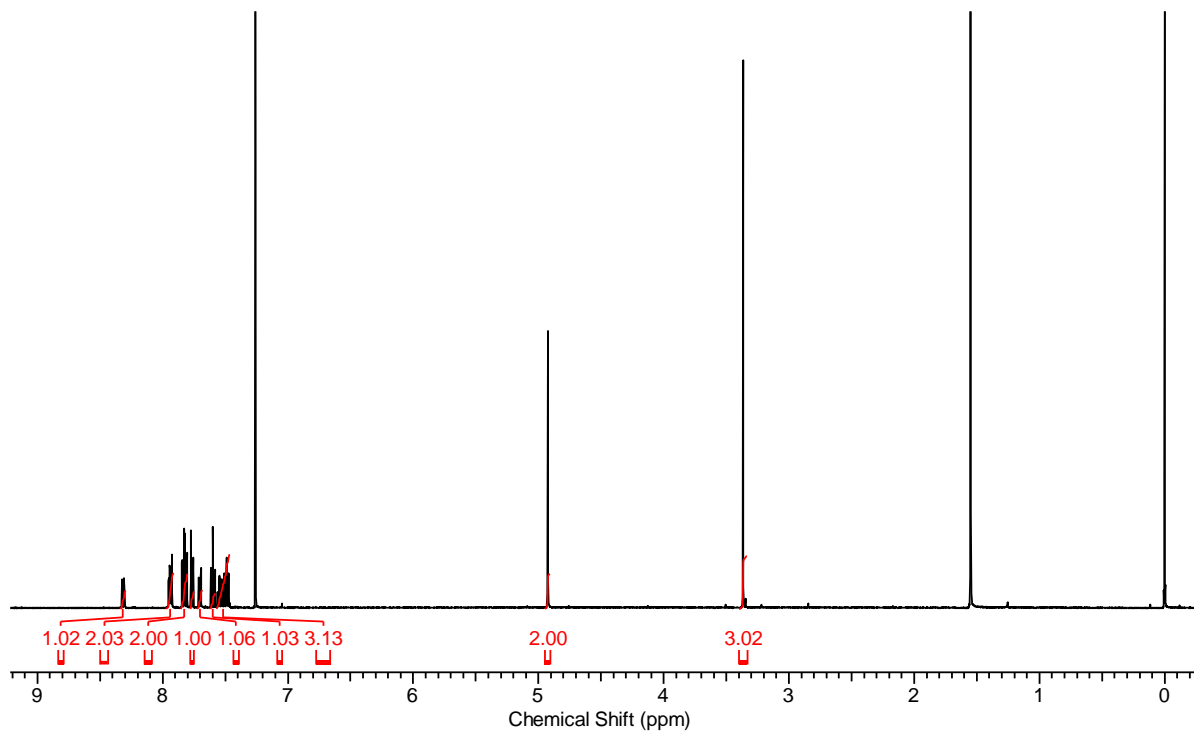


(S)/(R)-1: m.p. 244–248 °C; IR (KBr): 1604 cm^{-1} (C=N); ^1H NMR (CDCl_3 , 500 MHz) δ = 8.75 (d, J = 9.7 Hz, 1H, (*S,M*)), 8.73 (d, J = 9.5 Hz, 1H, (*S,P*)), 8.45 (d, J = 8.2 Hz, 1H, (*S,M*)), 8.40 (d, J = 8.5 Hz, 1H, (*S,P*)), 8.40 (s, 1H, (*S,P*)), 8.20 (s, 1H, (*S,M*)), 8.04–7.83 (m, 10H, (*S,P*) and (*S,M*)), 7.75–7.53 (m, 14H, (*S,P*) and (*S,M*)), 7.49–7.26 (m, 12H, (*S,P*) and (*S,M*)), 7.25–7.06 (m, 8H, (*S,P*) and (*S,M*)), 6.54 (d, J = 6.4 Hz, 2H, (*S,P*) and (*S,M*)), 6.43 (q, J = 6.8 Hz, 1H, (*S,P*)), 6.37 (q, J = 6.9 Hz, 1H, (*S,M*)), 2.08 (d, J = 6.9 Hz, 3H, (*S,M*)), 2.07 ppm (d, J = 6.8 Hz, 1H, (*S,P*)); ^{13}C NMR (CDCl_3 , 125 MHz) δ = 167.9, 167.8, 164.1, 163.9, 160.6, 159.9, 148.1, 148.0, 144.6, 143.4, 142.71, 142.69, 142.68, 138.39, 138.37, 138.34, 138.33, 137.2, 134.8, 134.61, 134.59, 132.61, 132.56, 132.53, 132.48, 131.6, 131.5, 130.89, 130.86, 130.6, 129.81, 129.75, 129.70, 129.6, 129.54, 129.52, 129.3, 129.2, 129.00, 128.96, 128.9, 128.7, 127.81, 127.59, 127.55, 127.31, 127.26, 127.23, 127.18, 126.92, 126.90, 126.81, 126.75, 126.6, 126.5, 126.04, 126.02, 126.00, 125.97, 125.10, 125.05, 124.20, 124.16, 124.1, 124.03, 124.00, 122.61, 122.49, 118.14, 118.09, 118.06, 118.0, 115.0, 114.68, 114.65, 114.5, 68.5, 68.4, 24.1, 22.3 ppm; HRMS (APCI+): m/z [M+H]⁺ calcd for $\text{C}_{42}\text{H}_{31}\text{N}_2\text{OPt}$: 774.2082; found: 774.2060; (*S*)-**1**: $[\alpha]_D^{25} = -32$ (*c* 0.001, CHCl_3), (*R*)-**1**: $[\alpha]_D^{25} = +31$ (*c* 0.001, CHCl_3).

(S)/(R)-2: m.p. 183–185 °C; IR (KBr): 1604 cm⁻¹ (C=N); ¹H NMR (CDCl₃, 500 MHz) δ = 9.34 (d, *J* = 6.4 Hz, 1H), 8.84 (d, *J* = 8.9 Hz, 1H), 8.04–7.99 (m, 1H), 7.91 (s, 1H), 7.88 (d, *J* = 8.2 Hz, 1H), 7.79–7.74 (m, 1H), 7.68 (ddd, *J* = 8.5, 6.9, 1.4 Hz, 1H), 7.61 (m, 1H), 7.56–7.51 (m, 3H), 7.42–7.34 (m, 3H), 7.33–7.12 (m, 1H), 7.17–7.12 (m, 2H), 7.10 (dd, *J* = 7.9, 1.8 Hz, 1H), 7.06 (d, *J* = 8.2 Hz, 1H), 6.53–6.48 (m, 1H), 6.32 (q, *J* = 7.0 Hz, 1H), 1.98 ppm (d, *J* = 7.0 Hz, 3H); ¹³C NMR (CDCl₃, 125 MHz) δ = 166.3, 160.8, 148.0, 143.4, 138.0, 137.7, 134.9, 134.6, 133.7, 131.3, 129.8, 129.6, 128.9, 128.0, 127.7, 127.6, 127.5, 127.46, 127.4, 126.9, 125.4, 122.8, 122.7, 122.2, 118.6, 115.0, 68.7, 23.4 ppm; HRMS (APCI+): m/z [M+H]⁺ calcd for C₃₀H₂₅N₂OPt: 624.1612; found: 624.1598; Anal. calcd for C₃₀H₂₄N₂OPt: C, 57.78; H, 3.88; N, 4.49; Found: C, 57.98; H, 3.68; N, 4.53; (*S*)-2: [α]_D²⁵ = -24 (*c* 0.001, CHCl₃), (*R*)-2: [α]_D²⁵ = +23 (*c* 0.001, CHCl₃).



(a)



(b)

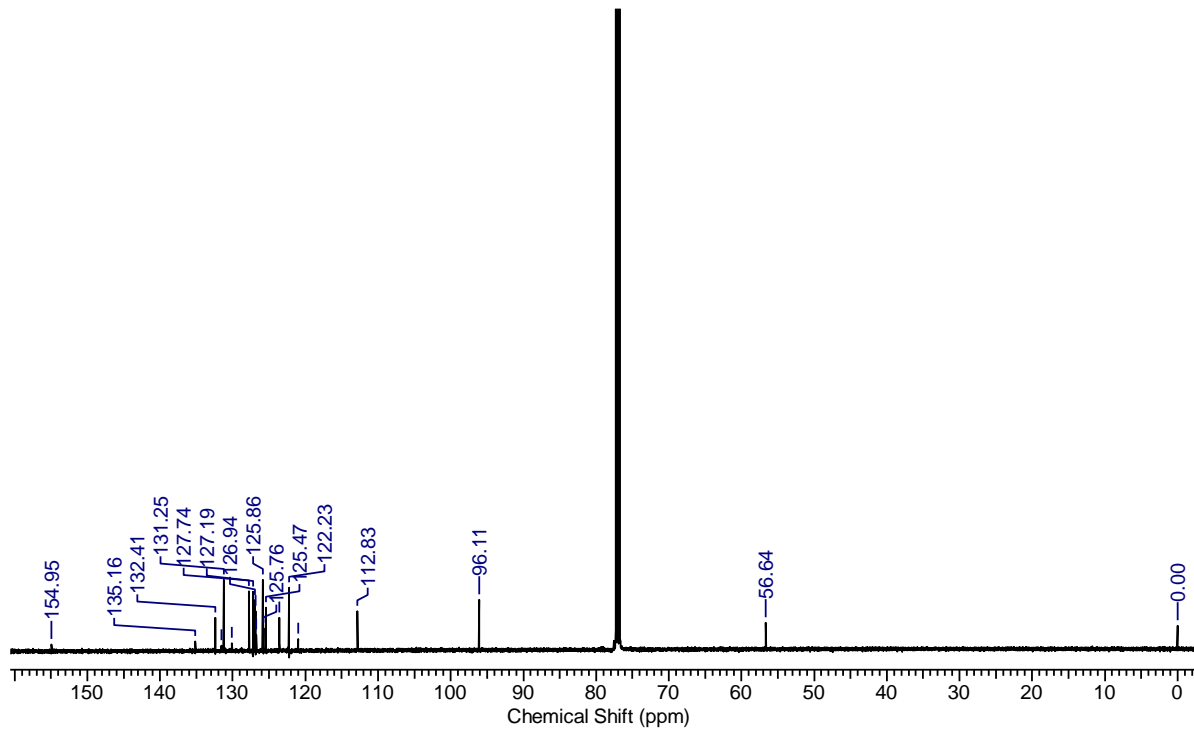
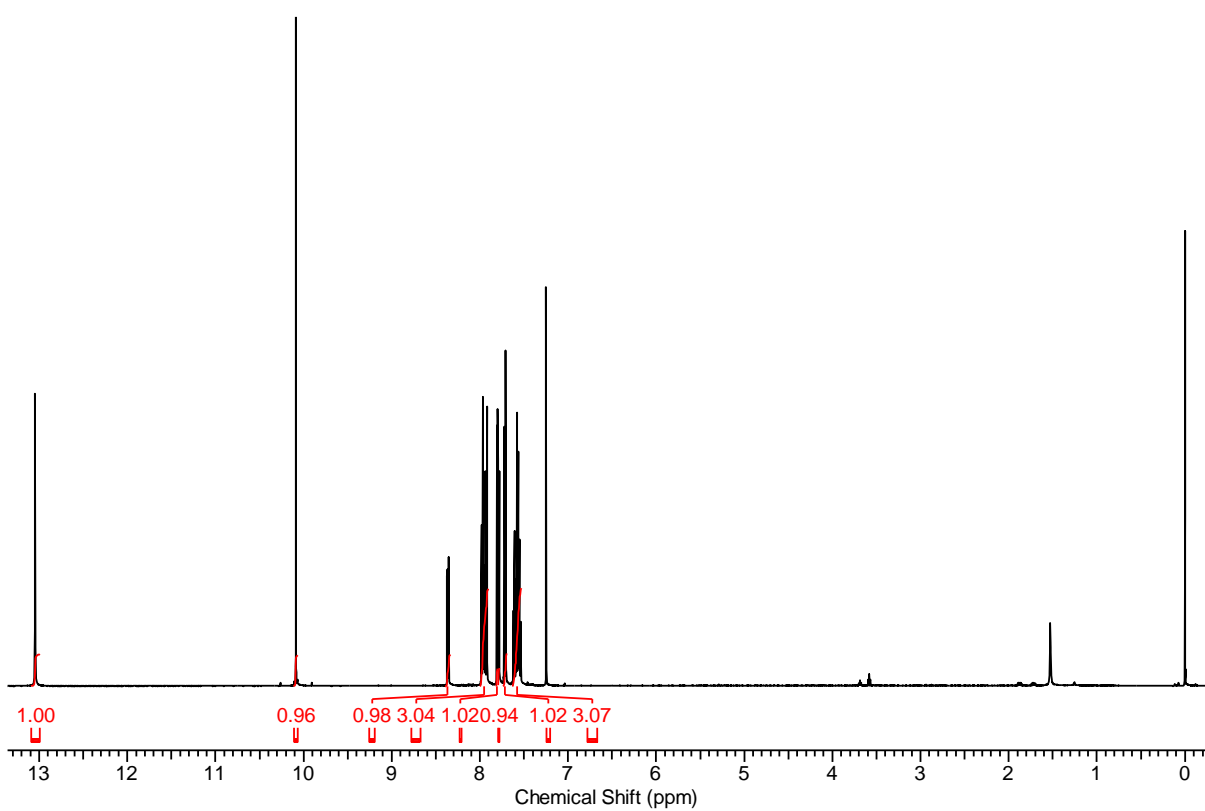


Fig. S1 (a) ¹H and (b) ¹³C NMR spectra of 1-(methoxymethoxy)benzo[c]phenanthrene (**4**) in CDCl₃.

(a)



(b)

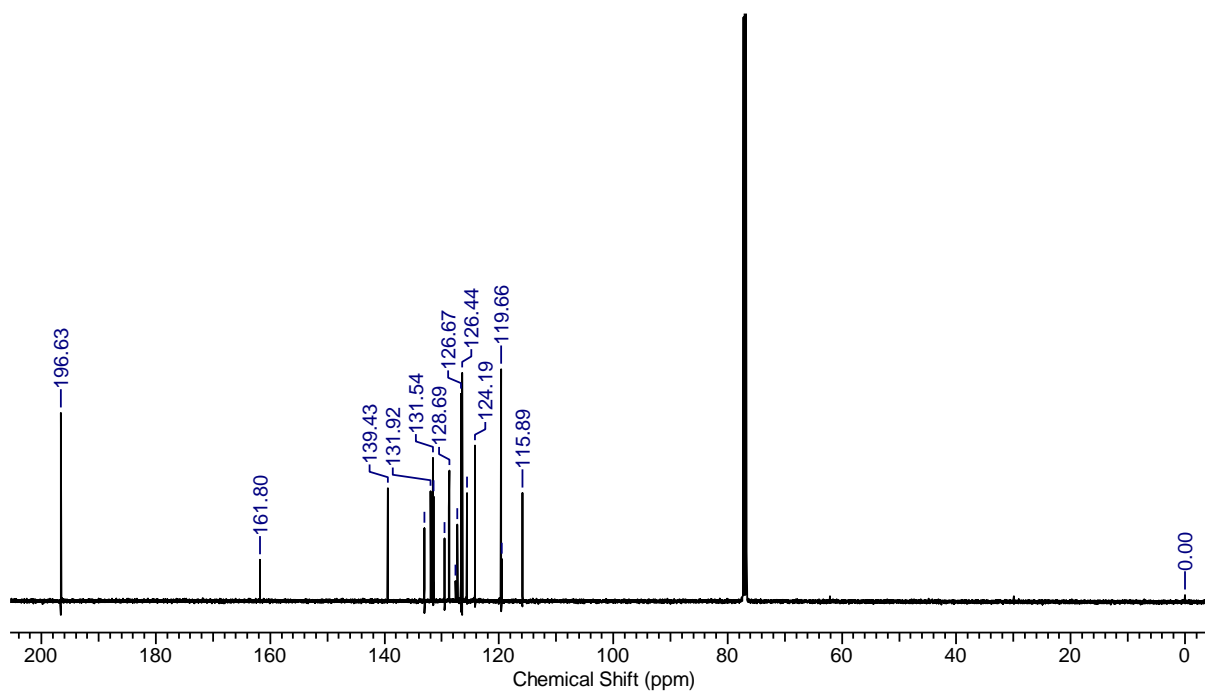
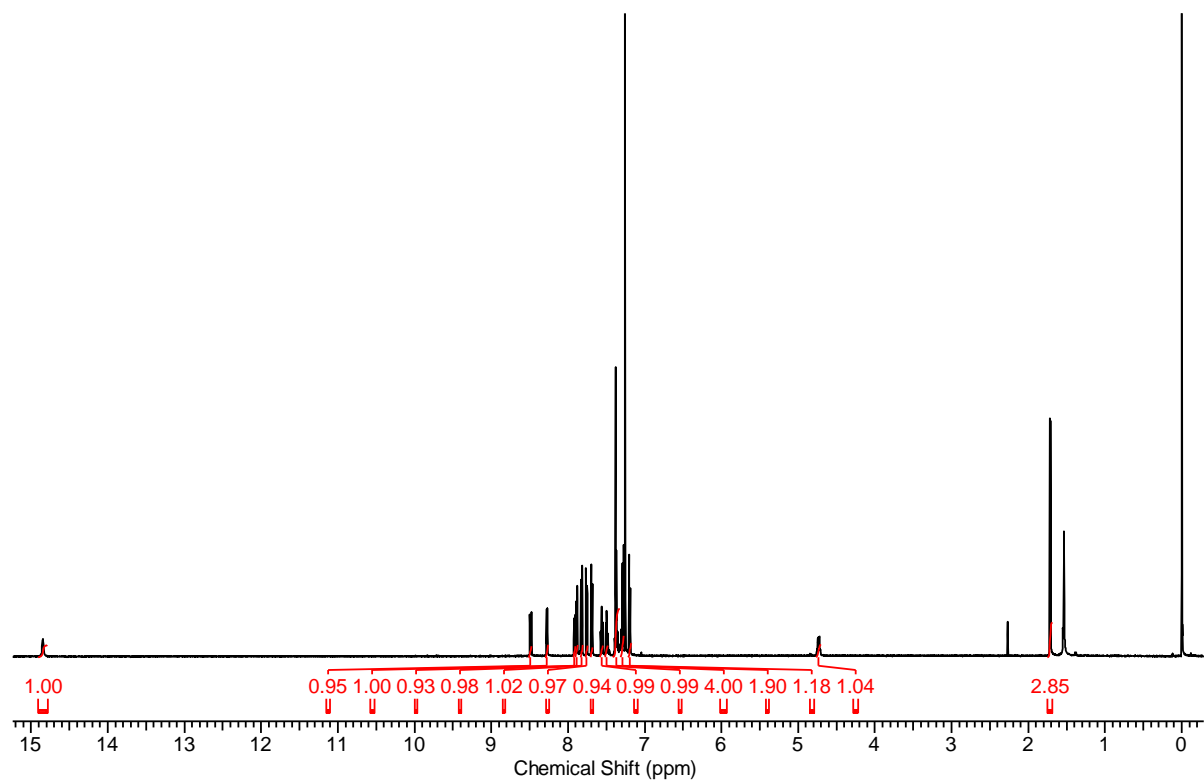


Fig. S2 (a) ¹H and (b) ¹³C NMR spectra of 1-hydroxybenzo[c]phenanthrene-2-carbaldehyde (**6**) in CDCl₃.

(a)



(b)

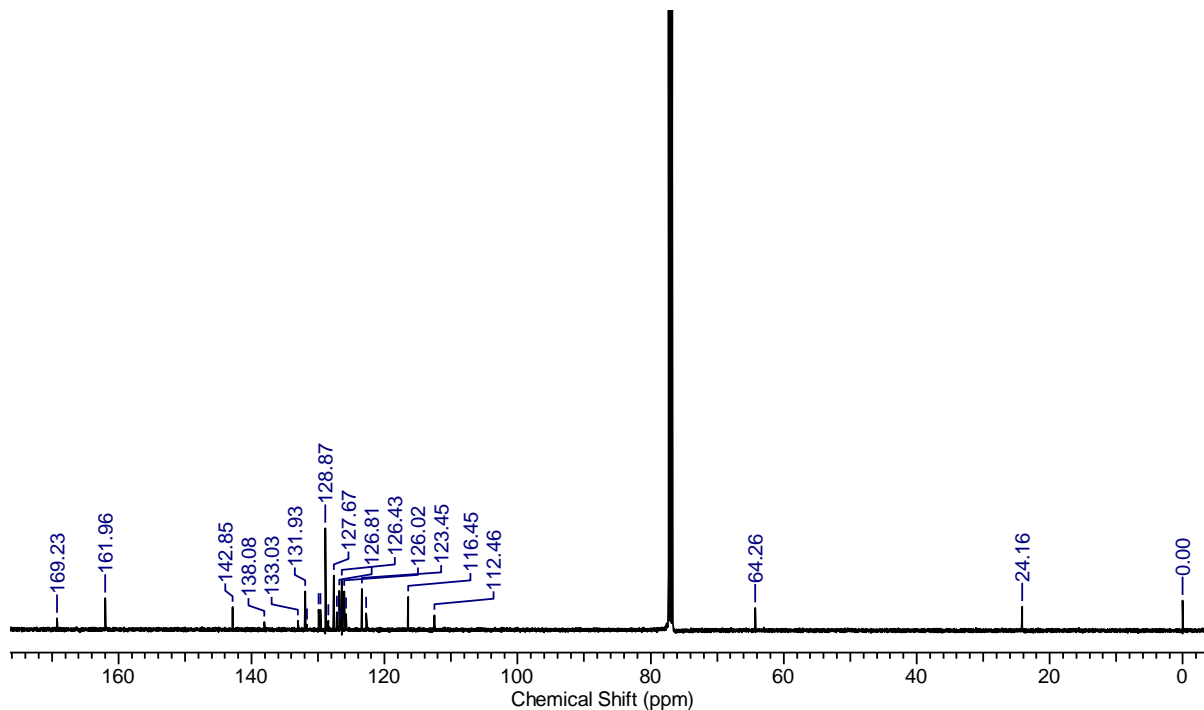
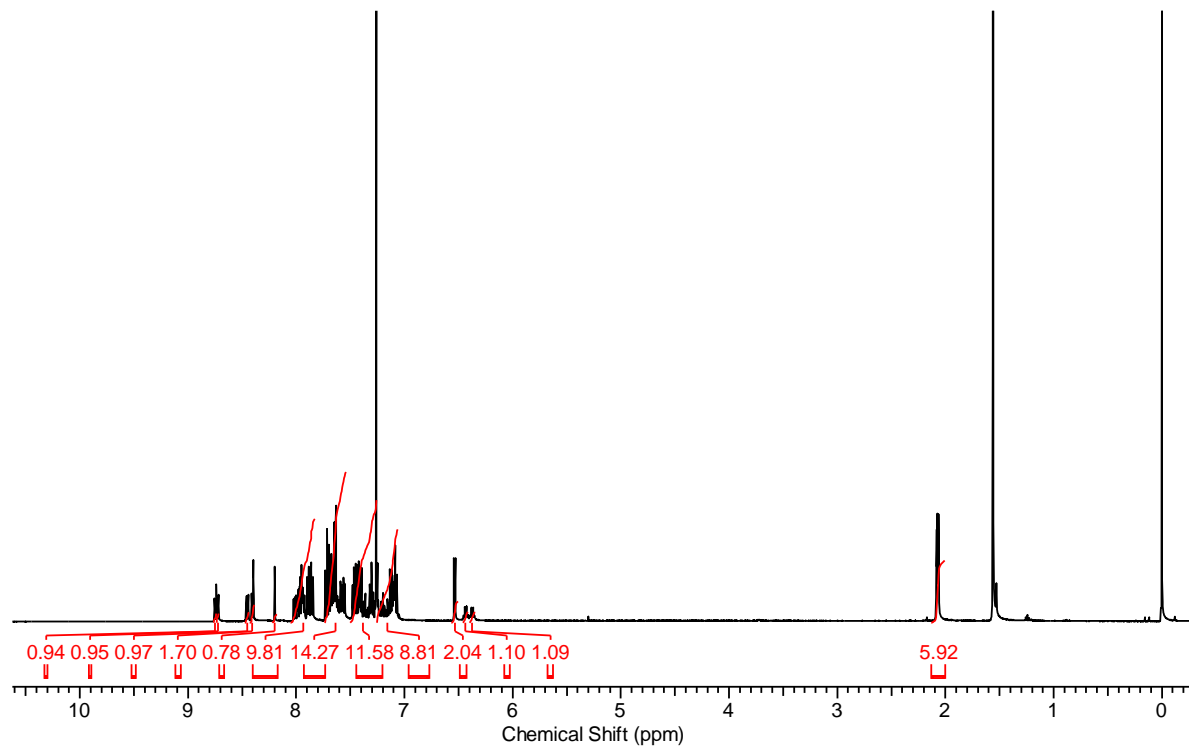


Fig. S3 (a) ¹H and (b) ¹³C NMR spectra of (S)-2-(((1-phenylethyl)imino)methyl)benzo[c]phenanthren-1-ol (**L1**) in CDCl₃.

(a)



(b)

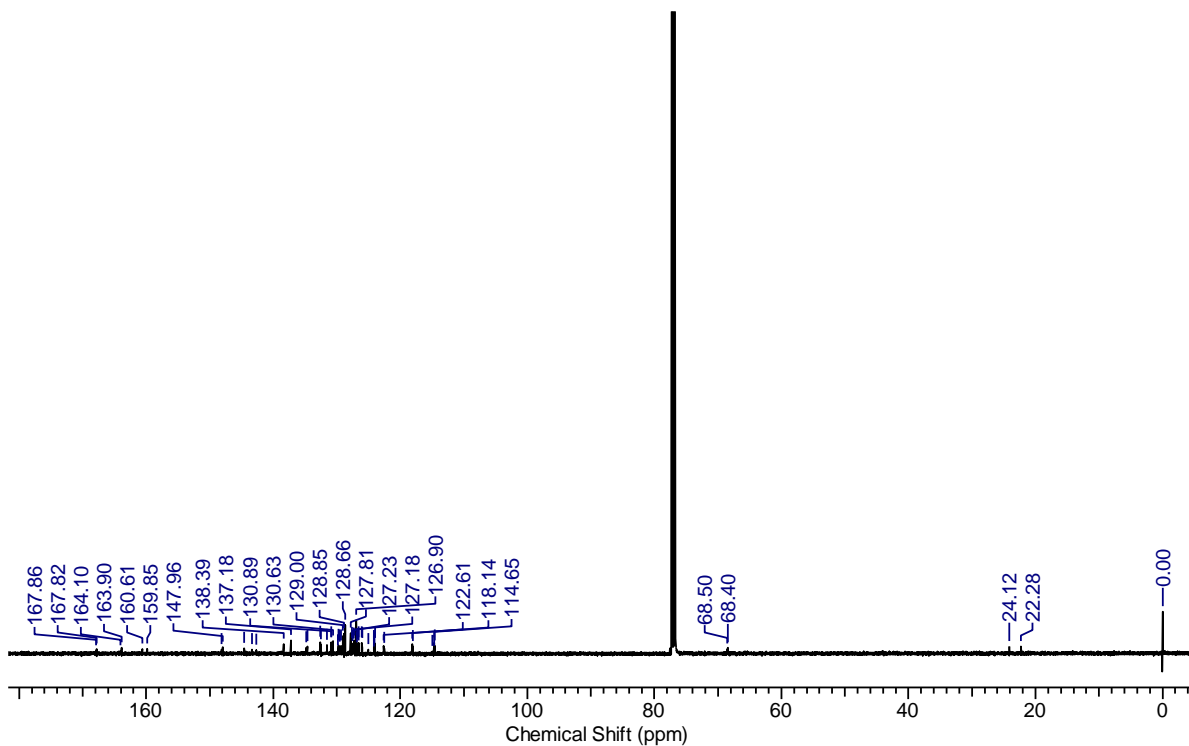
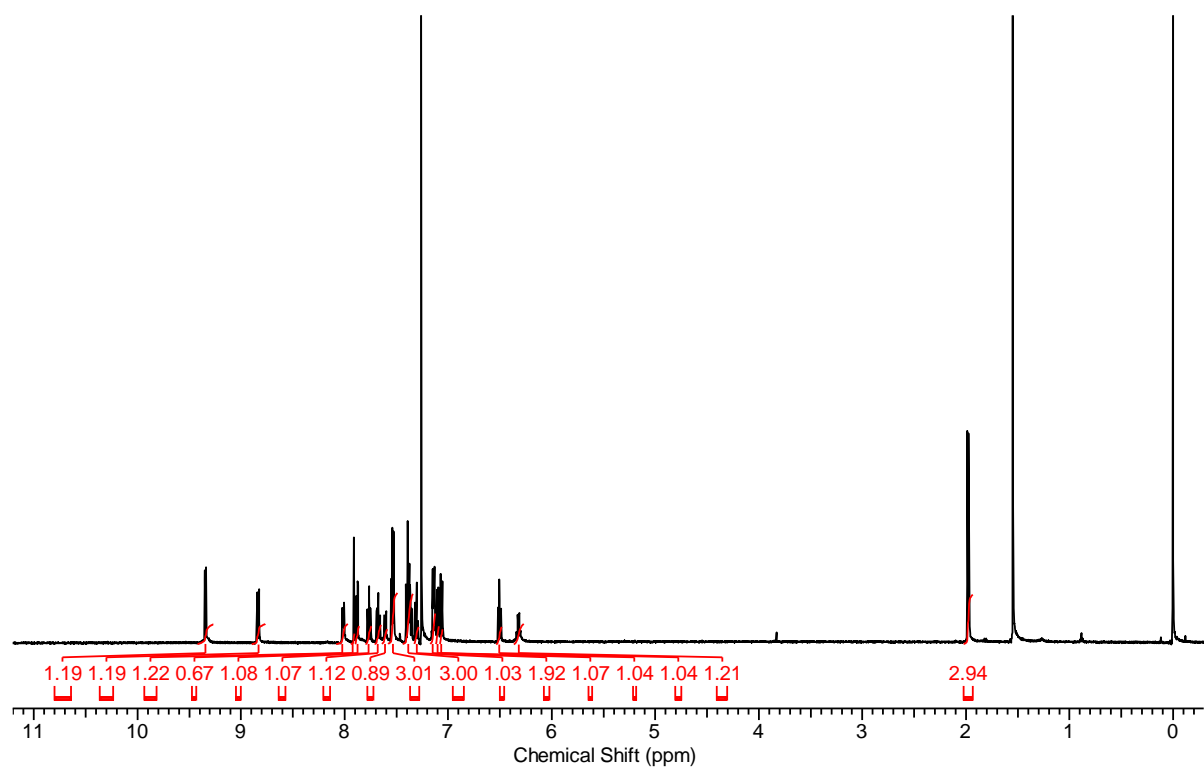


Fig. S4 (a) ^1H and (b) ^{13}C NMR spectra of (*S*)-**1** in CDCl_3 .

(a)



(b)

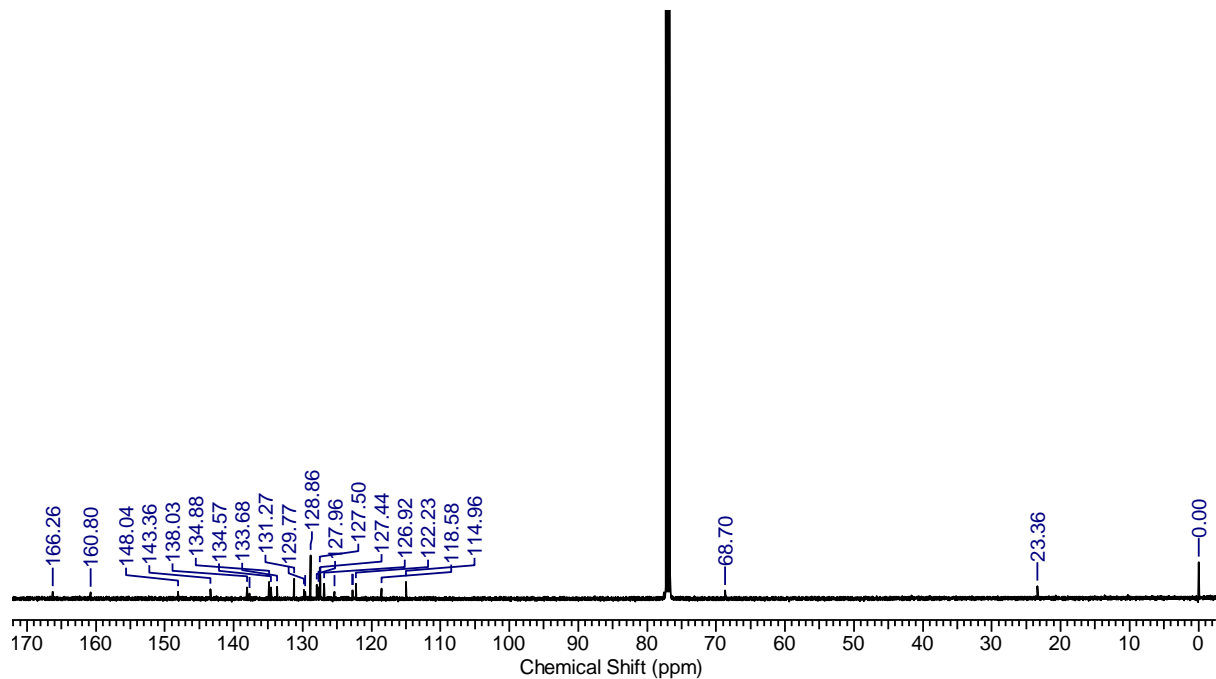


Fig. S5 (a) ^1H and (b) ^{13}C NMR spectra of (S)-2 in CDCl_3 .

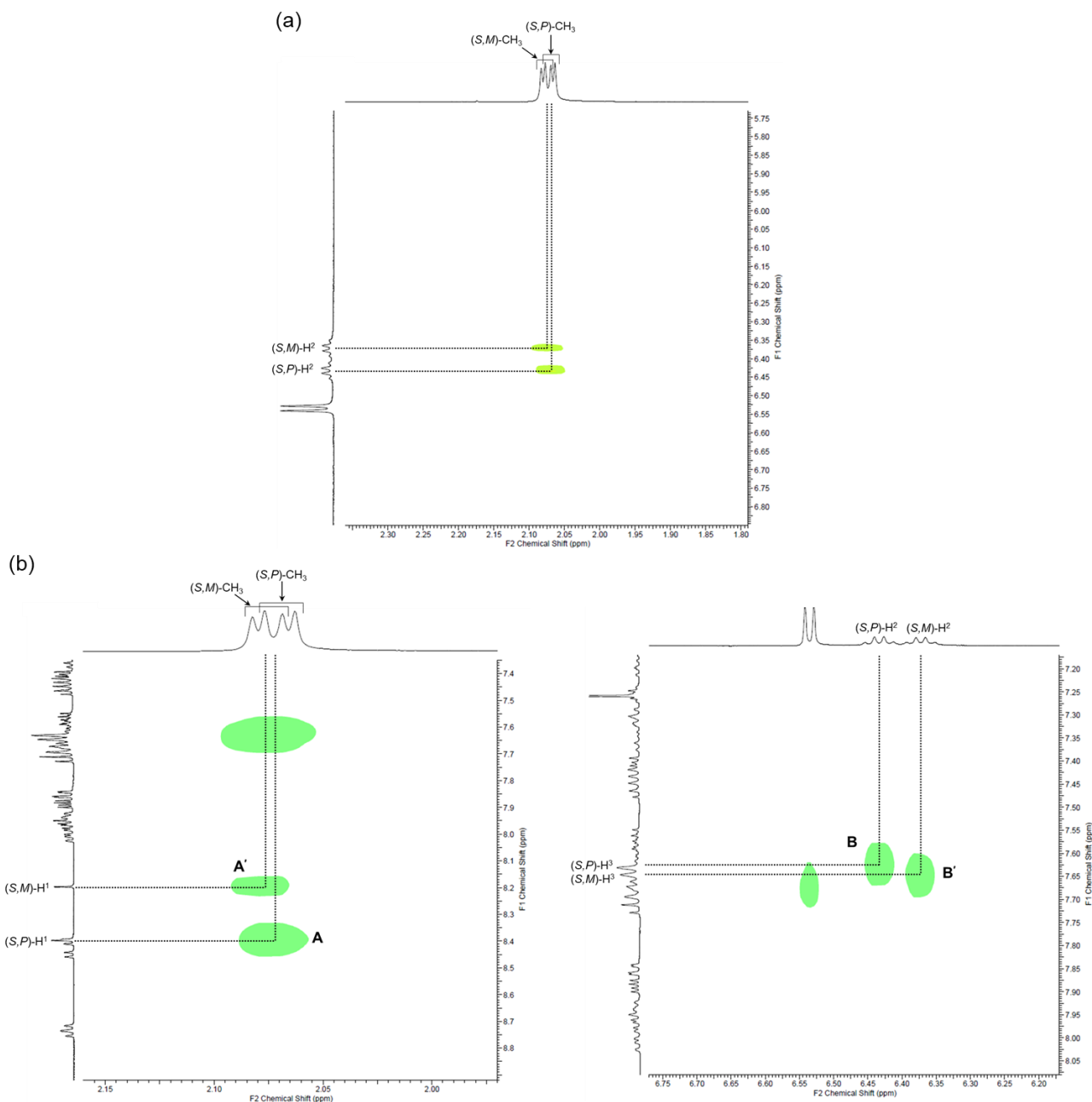
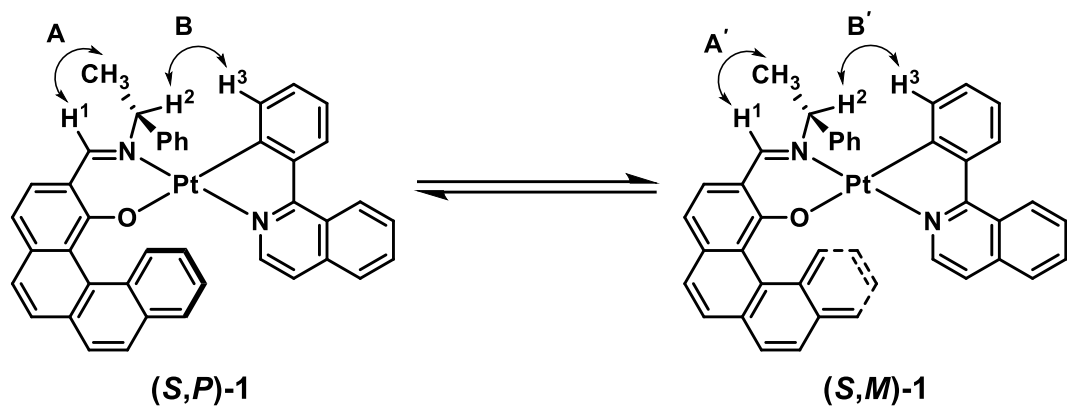


Fig. S6 (a) gCOSY and (b) NOESY spectra (500 MHz) of (S)-1 in CDCl_3 at 298 K.

3. Single Crystal X-ray Diffraction Analysis

Crystals suitable for XRD studies were analyzed using Rigaku XtaLAB mini2 benchtop X-ray crystallography system equipped with a Mo rotating-anode X-ray generator with monochromated Mo- K_{α} radiation ($\lambda = 0.71073 \text{ \AA}$). The molecular structures and packings in crystals *rac*-**1**, *rac*-**2**, were solved by direct methods and refined using the full-matrix least-squares method. In subsequent refinements, the function $\Sigma \omega(F_o^2 - F_c^2)^2$ was minimized, where F_o and F_c are the observed and calculated structure factor amplitudes, respectively. The positions of non-hydrogen atoms were found from differences in Fourier maps of electron density and refined anisotropically. All calculations were performed using the Crystal Structure crystallographic or CrysAlisPro program software package, and illustrations were drawn by using ORTEP.

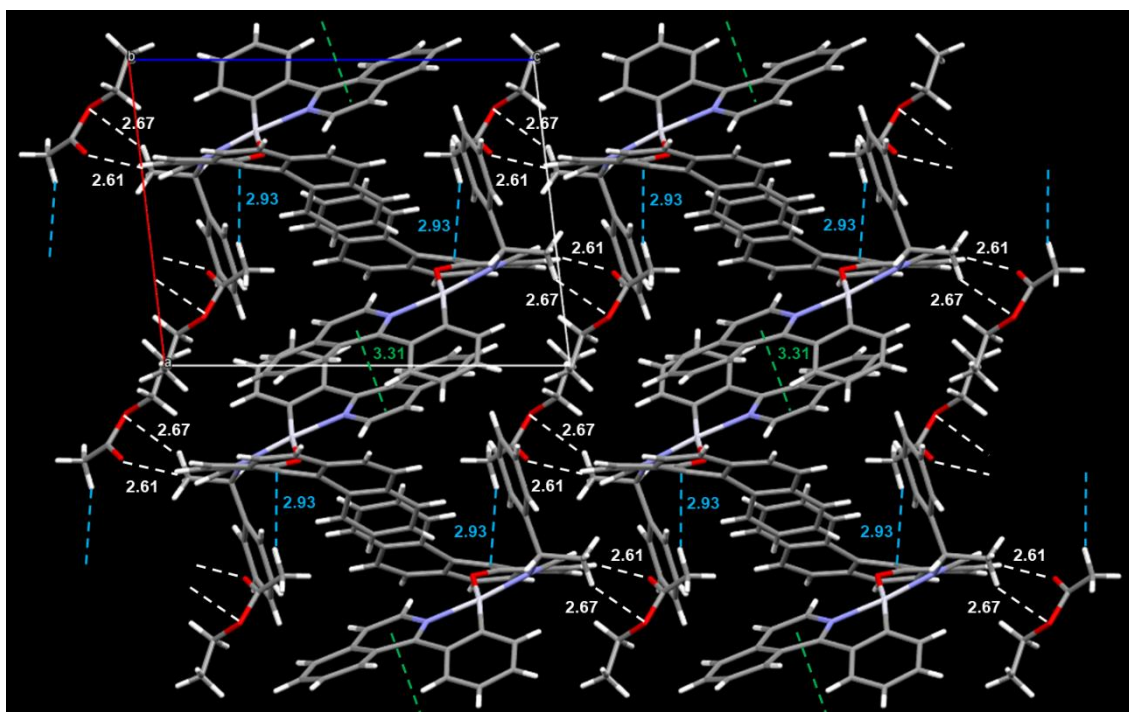


Fig. S7 Packing structure of *rac*-**1**. The *b*-axis projection showing CH- π (blue broken lines), π - π (green broken lines), and H··O (white broken lines) interactions.

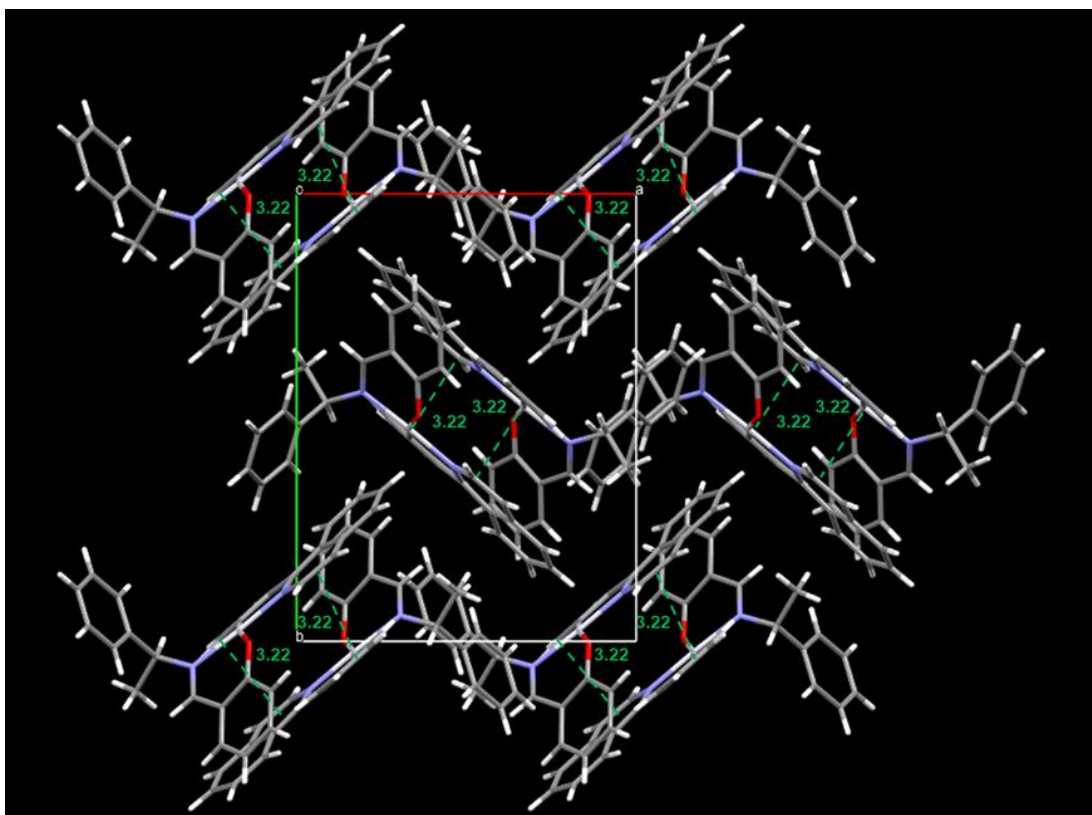


Fig. S8 Packing structure of *rac*-2. The *c*-axis projection showing π - π (green broken lines) interactions.

Table S1. Crystal data and structural refinement details for complexes *rac*-**1** and *rac*-**2**.

	<i>rac</i> - 1	<i>rac</i> - 2
Formula	C ₄₂ H ₃₀ N ₂ OPt·CH ₃ COOEt	C ₃₀ H ₂₄ N ₂ OPt
<i>M</i> _F	861.87	623.60
<i>T</i> [K]	113.15	113.15
Crystal color, habit	reddish colorless, block	reddish colorless, block
Crystal size [mm]	0.258×0.24×0.146	0.418×0.299×0.194
Crystal system	Triclinic	Monoclinic
Space group	<i>P</i> ī (#2)	<i>P</i> 2 ₁ /n (#14)
<i>a</i> [Å]	10.8643(3)	11.8288(4)
<i>b</i> [Å]	11.6179(5)	15.4199(5)
<i>c</i> [Å]	14.5758(8)	12.4090(4)
<i>α</i> [°]	77.263(4)	90
<i>β</i> [°]	82.321(3)	98.051(3)
<i>γ</i> [°]	84.958(3)	90
<i>V</i> [Å ³]	1775.15(13)	2241.08(13)
<i>Z</i>	2	4
<i>D</i> _{calcd} [g cm ⁻³]	1.612	1.848
Abs coeff (mm ⁻¹)	3.998	6.288
Abs correct	multi-scan	multi-scan
Transmiss max/min	1.0000/0.81892	1.0000/0.38036
<i>F</i> (000)	860	1216
θ range (°)	1.9500–26.9850	2.1400–29.7320
Rflns/unique	36661/10206	24394/6539
<i>R</i> _{int}	0.0844	0.0315
Data/params	10206/54/472	6539/0/308
Largest diff. peak and hole (e Å ⁻³)	8.129/–4.204	2.833/–1.290
<i>R</i> ₁ (<i>I</i> > 2σ(<i>I</i>)) ^[a]	0.0722	0.0303
w <i>R</i> ₂ (all reflections) ^[b]	0.1933	0.0605
Goodness of fit	1.080	1.030
CCDC No.	2321030	2321031

[a] $R_1 = \Sigma(|F_o| - |F_c|) / \Sigma(|F_o|)$. [b] $wR_2 = [\sum(w(F_o^2 - F_c^2)^2) / \sum(wF_o^2)^2]^{1/2}$.

4. NMR Analysis

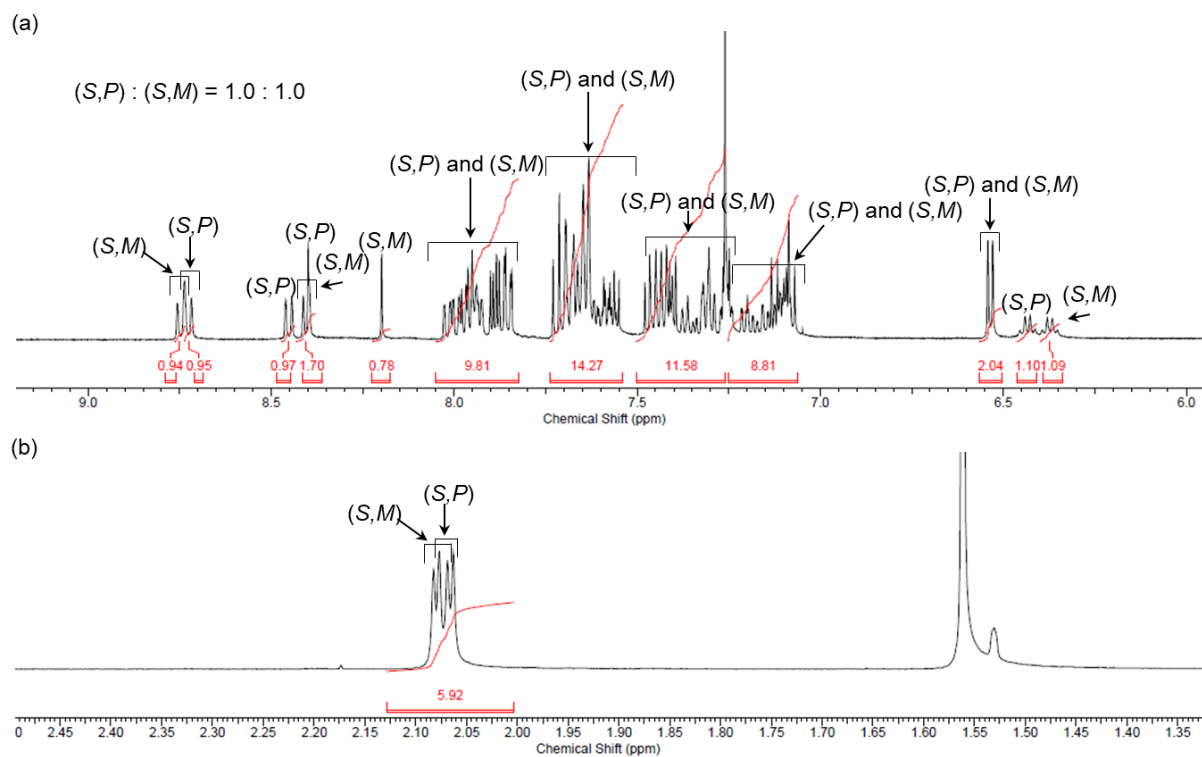


Fig. S9 ^1H NMR spectra of (a) aromatic and (b) aliphatic regions of (*S*)-**1** in CDCl_3 at 298 K.

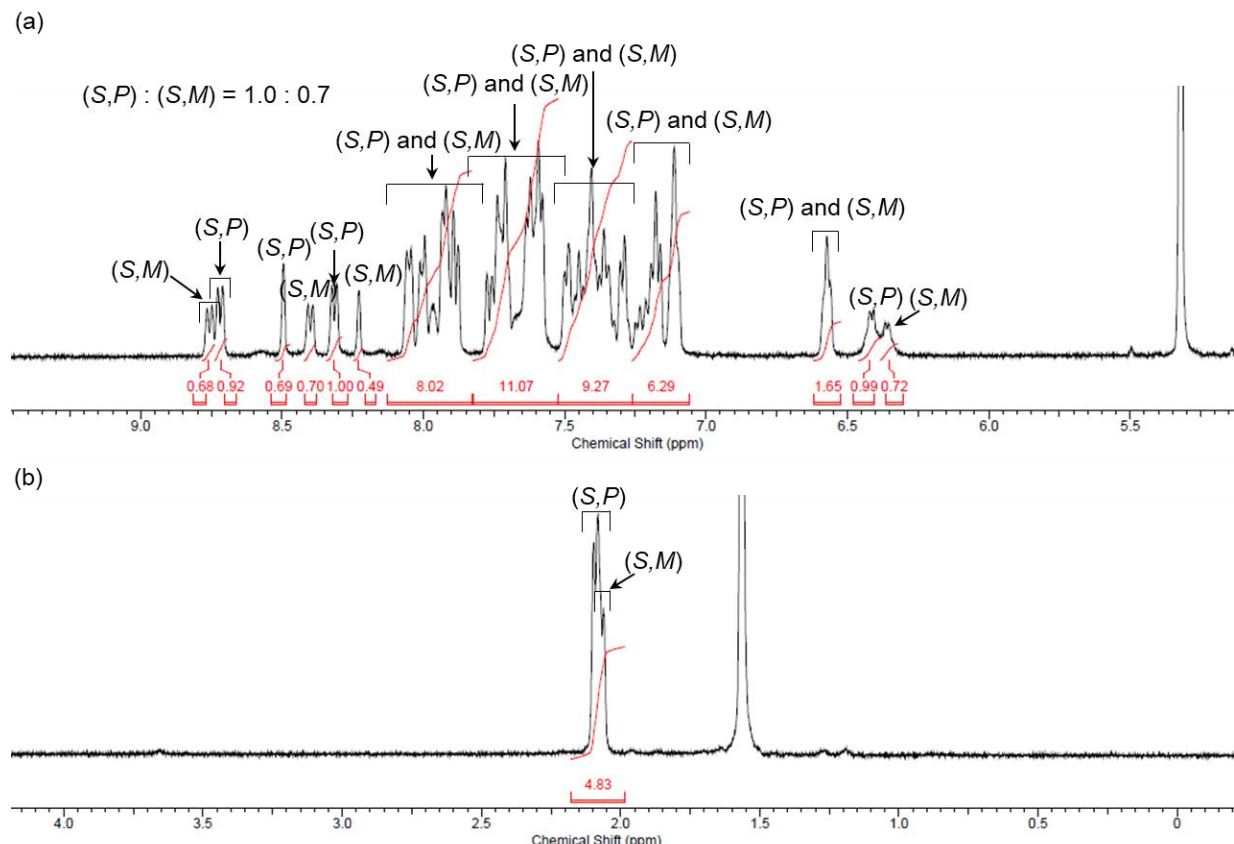
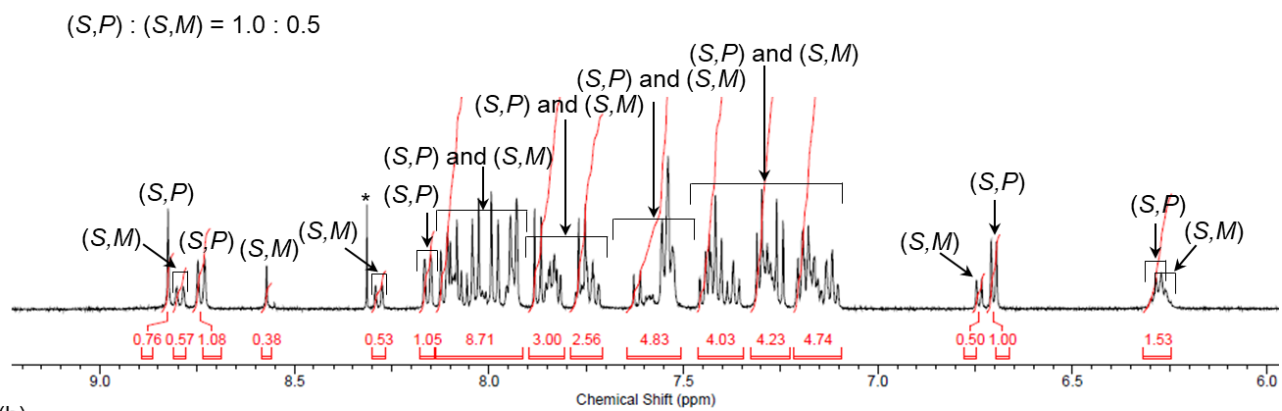


Fig. S10 ^1H NMR spectra of (a) aromatic and (b) aliphatic regions of (*S*)-**1** in CD_2Cl_2 at 298 K.

(a)



(b)

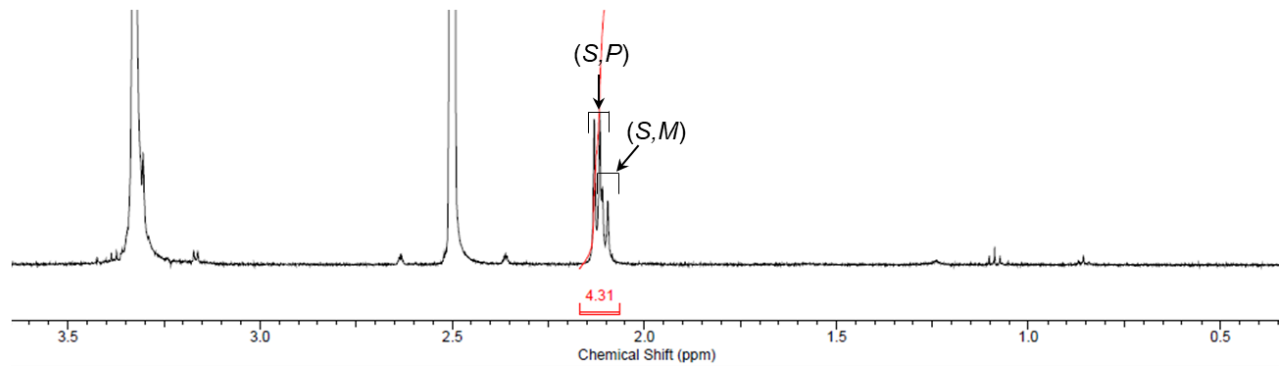


Fig. S11 ^1H NMR spectra of (a) aromatic and (b) aliphatic regions of (*S*)-**1** in $\text{DMSO}-d_6$ at 298 K. Asterisked peaks correspond to the CHCl_3 signal.

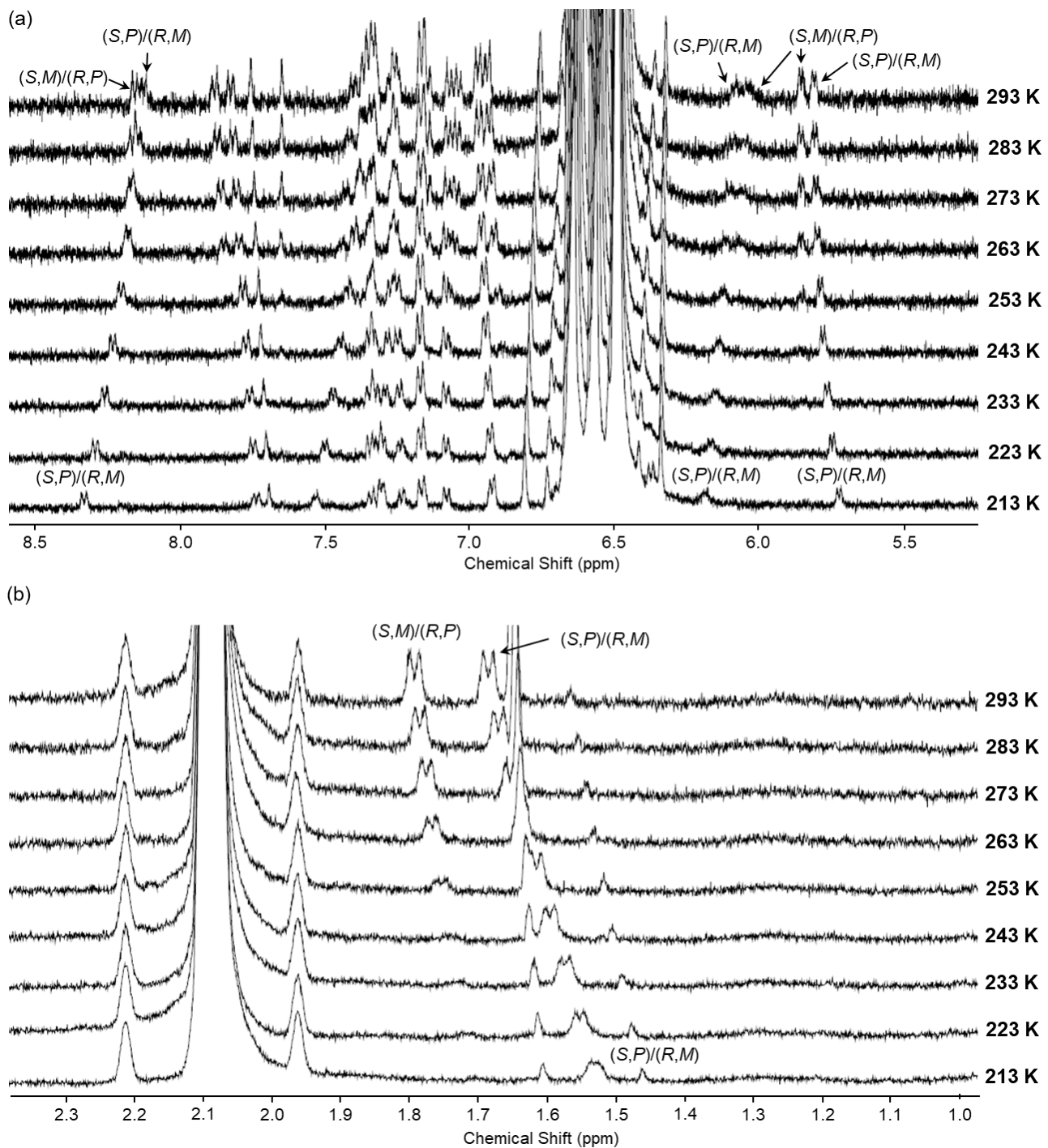


Fig. S12 VT ^1H NMR spectra (500 MHz) of (a) aromatic and (b) aliphatic regions of *rac*-**1** in toluene- d_8 . For these measurements, crystals of *rac*-**1** were dissolved in toluene- d_8 at 195 K and ^1H NMR spectra were recorded from 213 K to 293 K.

5. Photophysical Properties

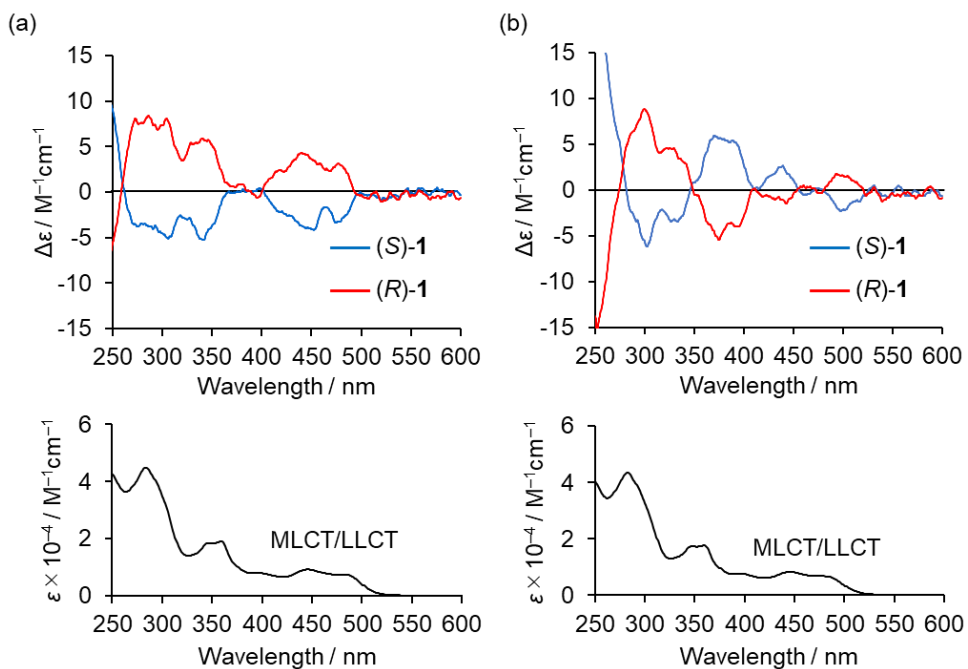


Fig. S13 CD (upper plot) and UV-vis (lower plot) spectra of **1** in (a) CHCl₃ and (b) DMSO (2.0×10^{-4} M) at 298 K.

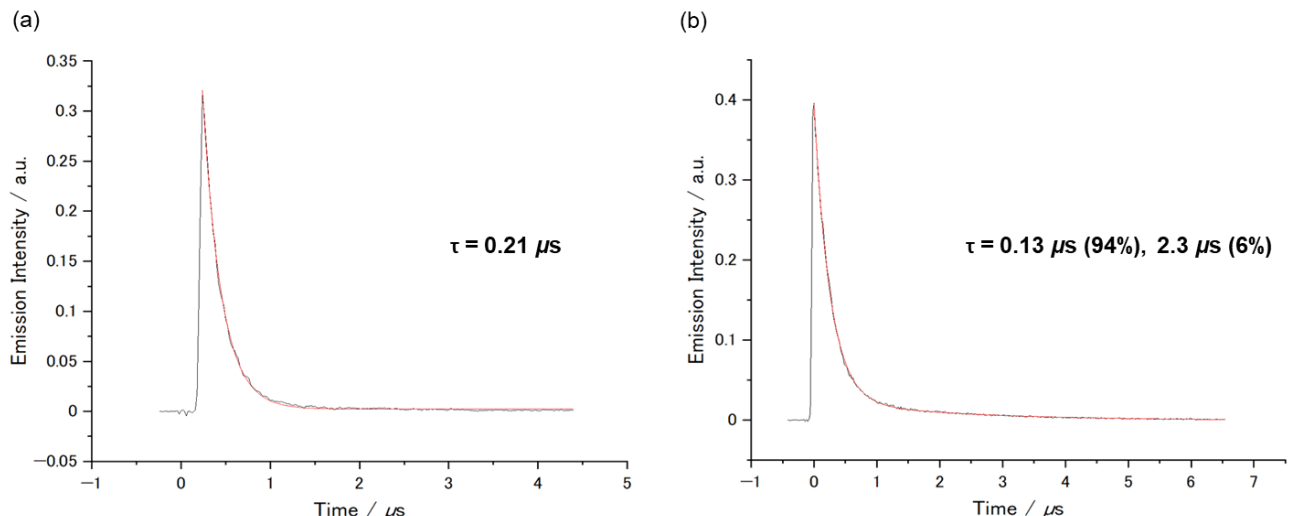


Fig. S14 Luminescence decay curve of (a) **1** and (b) **2** in CH₂Cl₂ (2.0×10^{-4} M) at 298 K.

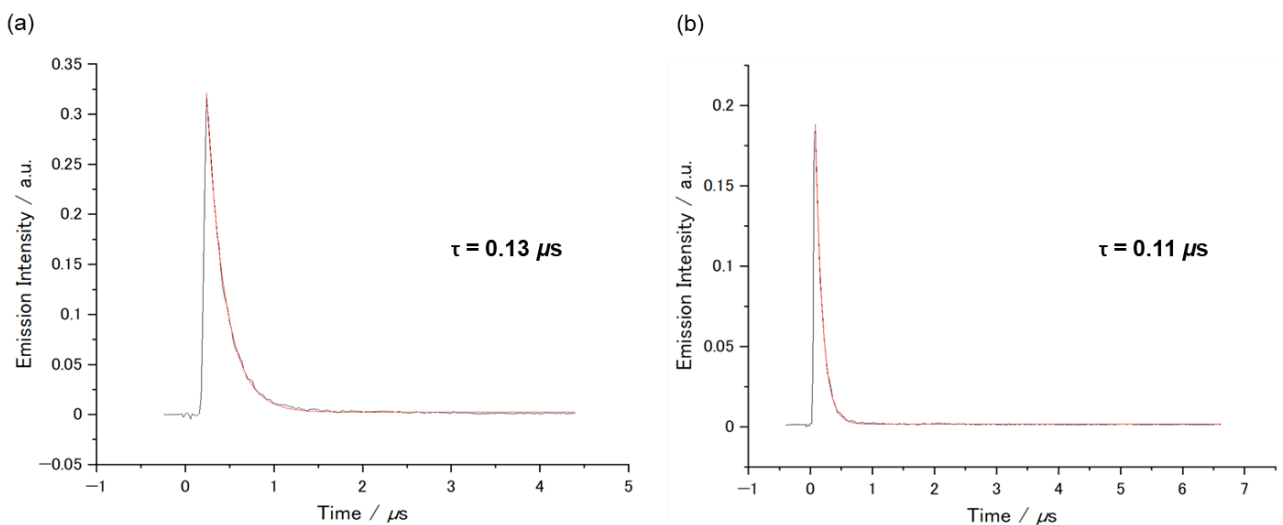


Fig. S15 Luminescence decay curve of **1** in (a) CHCl_3 and (a) DMSO ($2.0 \times 10^{-4} \text{ M}$) at 298 K.

Table S2. Photophysical data for complexes **1** and **2**.

Complex	Medium	λ_{abs} [nm] ^[a]	λ_{em} [nm] ^[b]	$\Phi^{[b,c]}$	τ [μs] ^[b]	$k_r \times 10^4 [\text{s}^{-1}]^{[d]}$	$k_{\text{nr}} \times 10^5 [\text{s}^{-1}]^{[e]}$	$ g_{\text{lum}} ^{[f]}$	$B_{\text{CPL}} [\text{M}^{-1}\text{cm}^{-1}]^{[h]}$
1	$\text{CH}_2\text{Cl}_2^{[a]}$	481	608	0.01	0.21	4.76	47.1	0.010	1.1
	$\text{CHCl}_3^{[a]}$	482	604	<0.01	0.13	4.23	76.5	— ^[g]	—
	DMSO ^[a]	478	604	0.01	0.11	9.09	90.0	— ^[g]	—
	solid	—	639	0.02	—	—	—	— ^[g]	—
2	$\text{CH}_2\text{Cl}_2^{[a]}$	460	607	0.02	0.13 (94%) 2.3 (6%)	7.69	37.7	0.003	0.3
	solid	—	632	0.06		—	—	— ^[g]	—

[a] Data were obtained from $2.0 \times 10^{-4} \text{ M}$ solutions at 298 K. [b] $\lambda_{\text{ex}} = 480$ (**1**), 470 (**2**) nm. [c] Luminescent quantum efficiencies measured using the absolute method with an integrating sphere. [d] $k_r = \Phi_{298\text{K}}/\tau$. [e] $k_{\text{nr}} = (1 - \Phi_{298\text{K}})/\tau$. [f] The average $|g_{\text{lum}}|$ values around λ_{max} . [g] CPP were not detected due to the low phosphorescence intensity. [h] $B_{\text{CPL}} = \varepsilon \times \Phi \times g_{\text{lum}}$.

6. Computational Methods

All calculations were carried out based on DFT with the B3LYP exchange-correlation functional, using the Gaussian 16W program package.^{S4} The basis set used was the effective core potential (LanL2DZ) for platinum atoms and 6-31G* for the remaining atoms. Molecular orbitals and their eigenvalues for (*S,P*)-**1** and (*S*)-**2** were estimated using the optimized geometries determined by the DFT calculations using initial geometries obtained from XRD analysis. An initial structure with opposite configuration at the metal, (*S,M*)-**1**, was obtained by mirror inversion of the optimized structure of (*S,P*)-**1**, followed by manual inversion of the carbon chirality centers only. The singlet–singlet ($E(S_n)$) and singlet–triplet ($E(T_n)$) transition energies were estimated by time-dependent (TD) DFT calculation (B3LYP/6-31G*, LanL2DZ).

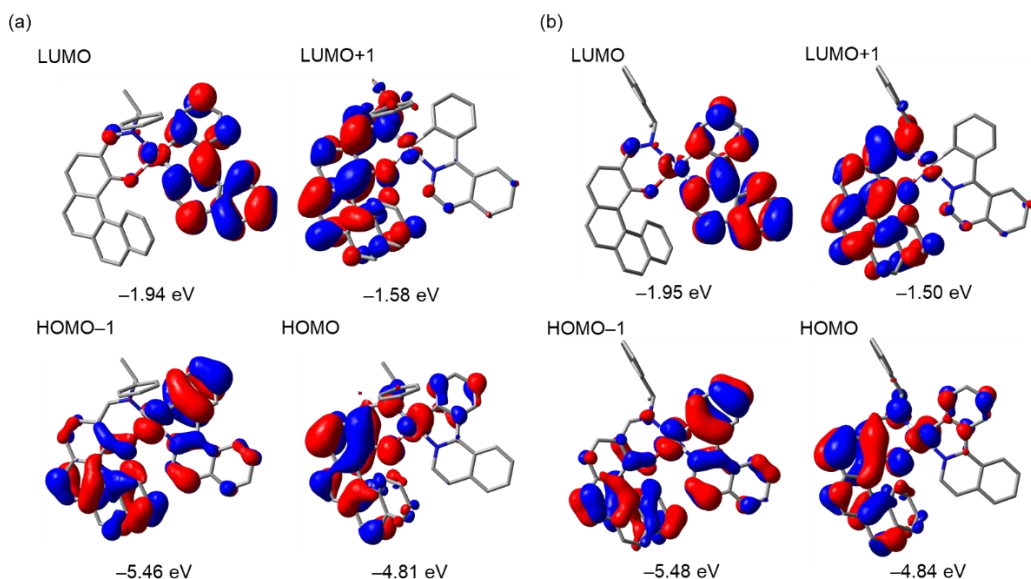


Fig. S16 Molecular orbitals and eigenvalues for the frontier orbitals of (a) (*S,P*)-**1** and (b) (*S,M*)-**1** estimated from DFT calculations (B3LYP/6-31G*, LanL2DZ) on the basis of the optimized geometries in the S_0 states.

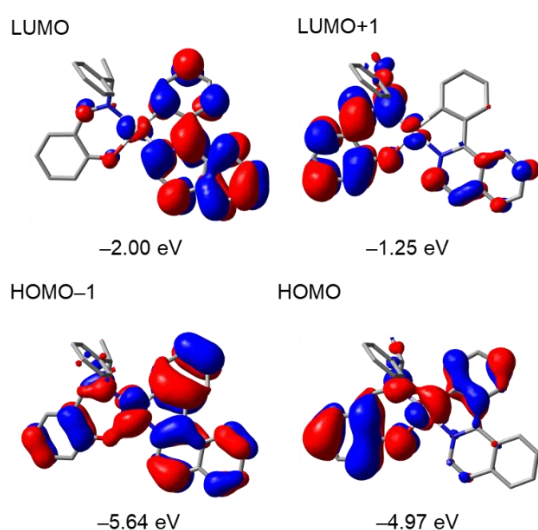


Fig. S17 Molecular orbitals and eigenvalues for the frontier orbitals of (*S*)-**2** estimated from DFT calculations (B3LYP/6-31G*, LanL2DZ) on the basis of the optimized geometries in the S_0 states.

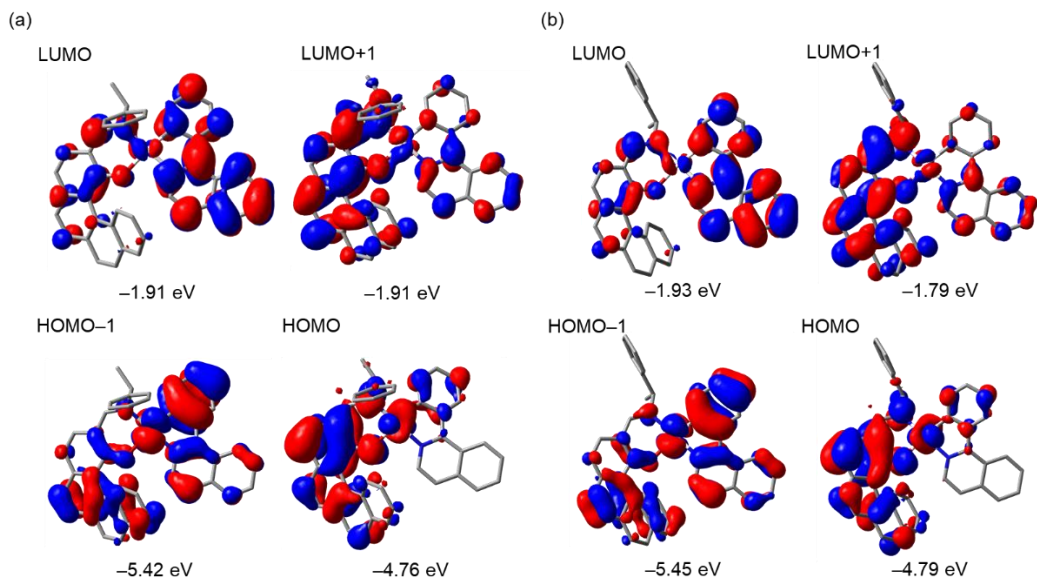


Fig. S18 Molecular orbitals and eigenvalues for the frontier orbitals of (a) (*S,P*)-**1** and (b) (*S,M*)-**1** estimated from DFT calculations (B3LYP/6-31G*, LanL2DZ) on the basis of the optimized geometries in the T₁ states.

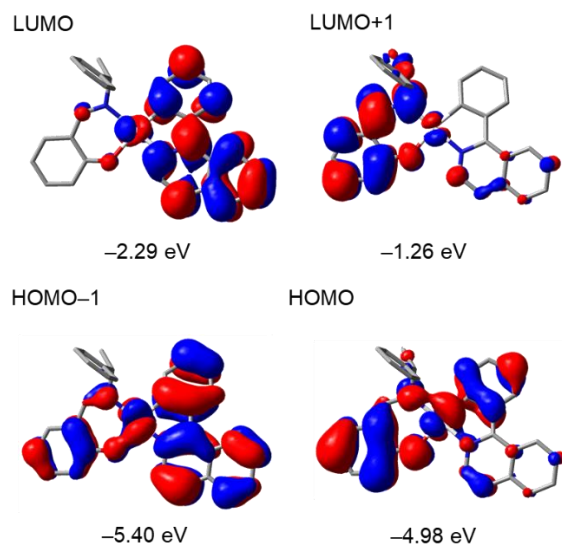


Fig. S19 Molecular orbitals and eigenvalues for the frontier orbitals of (*S*)-**2** estimated from DFT calculations (B3LYP/6-31G*, LanL2DZ) on the basis of the optimized geometries in the T₁ states.

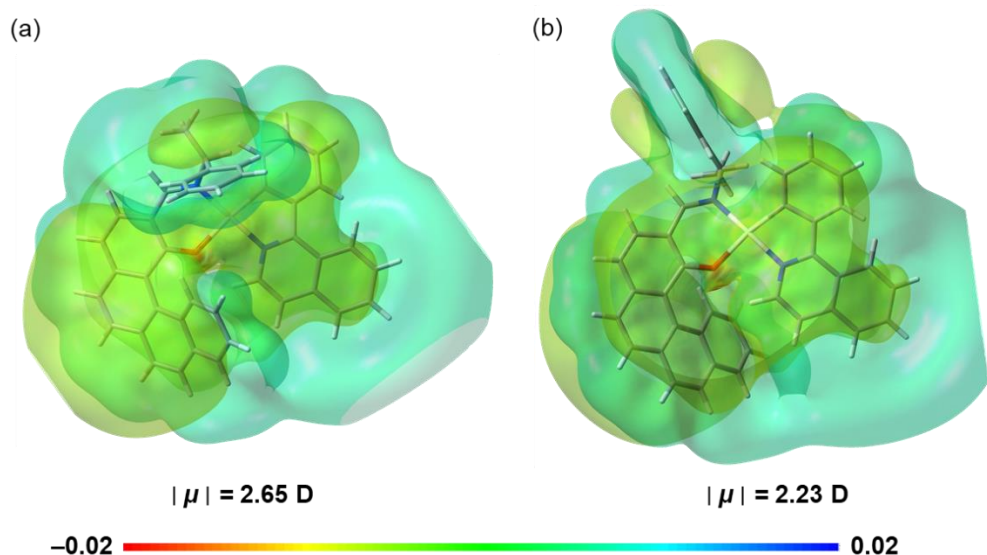


Fig. S20 Electrostatic potential (ESP) surfaces and dipole moments of (a) (*S,P*)-**1** and (b) (*S,M*)-**1** estimated from DFT calculations (B3LYP/6-31G*, LanL2DZ) on the basis of the optimized geometries in the S_0 optimized states.

Table S3. Selected data for excitation energy, major configuration, coefficient and oscillator strength for **1** and **2** (for the geometries optimized in the S_0 state).^[a]

Compound	State	Excitation energy [eV]	Major configuration ^[b]	Coefficient	Oscillator strength
(<i>S,P</i>)- 1	S_1	2.40 (518 nm)	HOMO→LUMO	0.697 (97%)	0.0554
	S_2	2.77 (448 nm)	HOMO→LUMO+1	0.684 (94%)	0.0762
(<i>S,M</i>)- 1	S_1	2.42 (511 nm)	HOMO→LUMO	0.697 (97%)	0.0596
	S_2	2.81 (441 nm)	HOMO→LUMO+1	0.676 (91%)	0.0893
(<i>S</i>)- 2	S_1	2.46 (503 nm)	HOMO→LUMO	0.695 (97%)	0.0729
	S_2	3.01 (411 nm)	HOMO→LUMO+1	0.650 (85%)	0.0596

[a] Estimated by TD-DFT (B3LYP/6-31G*, LanL2DZ) calculations based on the optimized geometries. [b] Molecular orbitals are shown in Fig. S16 and S17.

Table S4. Selected data for excitation energy, major configuration and coefficient for **1** and **2** (for the geometries optimized in the T_1 state).^[a]

Compound	State	Excitation energy [eV]	Major configuration ^[b]	Coefficient
(<i>S,P</i>)- 1	T_1	2.08 (597 nm)	HOMO→LUMO	0.616 (76%)
(<i>S,M</i>)- 1	T_1	2.11 (589 nm)	HOMO→LUMO+1	0.613 (75%)
			HOMO→LUMO	0.287 (16%)
(<i>S</i>)- 2	T_1	2.17 (571 nm)	HOMO→LUMO	0.521 (54%)

[a] Estimated by TD-DFT (B3LYP/6-31G*, LanL2DZ) calculations based on the optimized geometries. [b] Molecular orbitals are shown in Fig. S18 and S19.

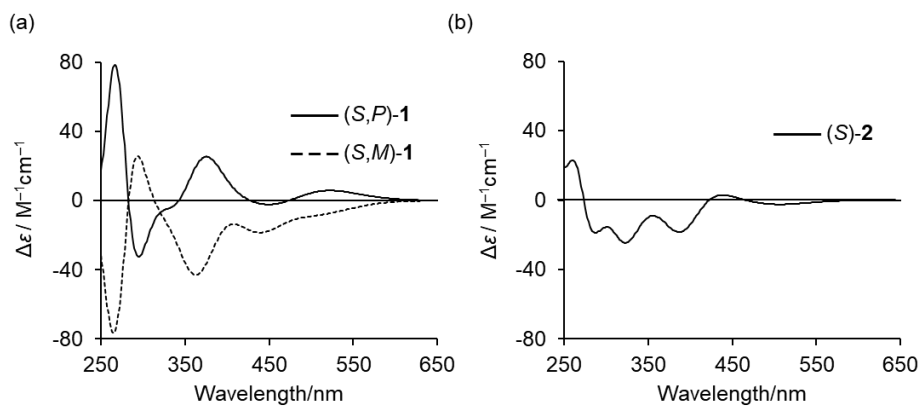


Fig. S21 Theoretical CD spectra of (a) (*S*)-**1** and (b) (*S*)-**2** estimated by TD-DFT calculation (B3LYP/6-31G*, LanL2DZ, Half-With = 0.2 eV).

Table S5. Peak information for theoretical CD spectra of (*S,P*)-**1**.^[a]

Wavelength [nm]	$\Delta\epsilon$ [$M^{-1}cm^{-1}$]	R_{vel} [$10^{-40} esu^2 cm^2$]
518.18	24.94	314.5
447.87	-15.81	-230.7
426.7	8.17	125.1
398.95	-8.12	-133.0
389.88	6.51	109.1
380.07	24.00	412.8
371.54	51.90	913.0
359.91	22.93	416.4
356.88	-6.30	-115.4
354.69	-33.07	-609.3
344.42	51.58	978.8
338.7	-70.42	-1359.0
333.38	25.42	498.4
327.21	2.97	59.3
323.37	-9.44	-190.9
316.55	3.69	76.2
309.55	-10.80	-228.0
307.45	93.75	1992.9
306.14	-91.35	-1950.2
303.83	2.79	60.0
302.27	-32.67	-706.4
299.38	16.16	352.8

295.34	3.39	75.0
294.75	7.91	175.5
292.06	-12.13	-271.5
290.48	-12.35	-278.0
289.8	-27.22	-614.0
287.63	-22.22	-504.9
286.48	-10.44	-238.2
285.74	16.92	387.0
284.28	2.20	50.6
283.8	-3.05	-70.2
281.51	-36.58	-849.3
277.76	-7.28	-171.3
276.06	15.20	359.8
275.62	-30.82	-730.9
274.16	7.59	181.0
273.56	65.36	1561.7
271.97	18.64	448.0
270.51	48.04	1160.7
269.31	4.81	116.8
266.86	-3.93	-96.2
266.35	7.83	192.1
264.41	90.09	2226.9
263.97	-56.38	-1396.1
263.64	14.10	349.7
262.19	24.32	606.4
260.64	-32.79	-822.3
258.28	75.05	1899.2
256.59	-35.88	-914.0

[a] Estimated by TD-DFT (B3LYP/6-31G*, LanL2DZ) calculations based on the optimized geometries.

Table S6. Peak information for theoretical CD spectra of (*S,M*)-**1**.^[a]

Wavelength [nm]	$\Delta\epsilon$ [$M^{-1}cm^{-1}$]	R_{vel} [$10^{-40} esu^2 cm^2$]
510.82	-28.68	-360.3
440.5	-50.66	-738.1
424.07	-14.64	-221.6
394.51	12.01	195.4
383.39	-4.06	-67.9
378.62	-24.80	-420.4
366.88	-61.49	-1075.7
358.22	-16.13	-288.9
353.26	-8.96	-162.8
351.34	-25.17	-459.7
338.63	10.75	203.8
337.84	-12.75	-242.3
332.88	-9.46	-182.4
324.63	-4.57	-90.4
320.69	3.41	68.3
313.31	-10.66	-218.4
309.03	0.54	11.3
307.66	-40.80	-851.0
305.05	83.46	1756.0
303.6	-35.16	-743.3
299.96	16.91	361.8
299.41	-12.57	-269.4
295.96	3.79	82.1
293.39	-2.34	-51.2
291.03	-12.47	-275.0
288.84	0.91	20.3
288.47	47.16	1049.2
287.5	-1.99	-44.4
285.77	8.50	190.9
283.55	62.79	1421.2
281.11	-0.50	-11.5
280.28	-1.60	-36.7
277.75	-22.75	-525.6
275.87	1.16	27.0

274.57	12.51	292.4
273.91	-83.63	-1959.6
273.27	-25.05	-588.3
271.23	0.41	9.6
269.39	40.70	969.6
268.92	-47.08	-1123.6
266.82	0.86	20.6
265.82	-16.70	-403.1
264.95	7.30	176.9
263.53	-5.93	-144.5
262.99	-47.42	-1157.2
261.65	-6.75	-165.7
260.5	41.16	1014.0
258.82	-43.47	-1077.8
257.24	-18.01	-449.3
256.91	-22.80	-569.6

[a] Estimated by TD-DFT (B3LYP/6-31G*, LanL2DZ) calculations based on the optimized geometries.

Table S7. Peak information for theoretical CD spectra of (S)-2.^[a]

Wavelength [nm]	$\Delta\epsilon$ [$M^{-1}cm^{-1}$]	R_{vel} [$10^{-40} esu^2 cm^2$]
503.49	-10.08	-117.7
411.33	53.56	765.1
396.82	-79.78	-1181.3
387.08	-11.31	-171.7
353.73	-8.39	-139.3
350.92	-1.63	-27.2
338.51	8.23	142.9
326.8	-49.86	-896.6
316.54	-11.54	-214.3
314.1	-1.55	-29.0
310.94	-11.38	-215.0
302.7	10.35	200.9
297.19	-1.33	-26.3
296.74	3.93	77.8
294.76	-2.64	-52.6
292.61	-23.14	-464.7
286.81	1.84	37.8
284.04	-5.23	-108.2
283.54	-9.92	-205.6
281.13	-0.34	-7.0
280.48	-5.59	-117.2
277.91	13.18	278.7
275.42	-26.80	-571.8
274.89	-8.27	-176.9
273.88	4.42	94.9
270.75	-14.63	-317.4
267.37	-41.95	-922.0
266.55	90.31	1990.7
263.4	3.76	83.9
261.59	2.87	64.6
260.55	20.53	463.0
259.04	0.27	6.0
255.95	-8.92	-204.7
251.76	-1.34	-31.2

247.68	-1.64	-38.9
244.41	7.58	182.2
244.03	26.59	640.3
243.4	-24.14	-582.7
242.92	26.81	648.6
241.65	11.89	289.1
241.27	-19.49	-474.7
240.66	-6.45	-157.6
238.81	-2.14	-52.7
236.33	14.36	357.1
235.87	-23.11	-575.8
234.49	7.47	187.2
234.12	46.24	1160.6
233.67	11.04	277.7
231.95	-12.61	-319.5
231.12	4.70	119.5

[a] Estimated by TD-DFT (B3LYP/6-31G*, LanL2DZ) calculations based on the optimized geometries.

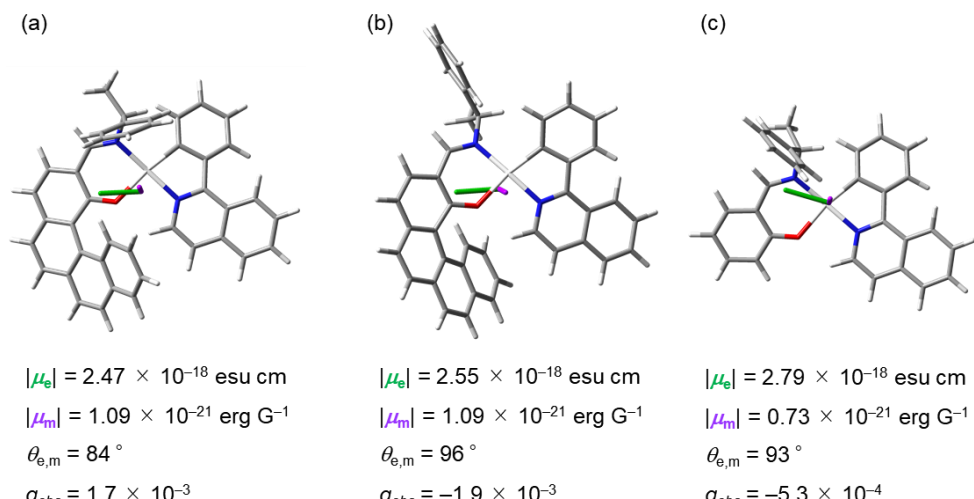


Fig. S22 Electric (μ_e , orange) and magnetic (μ_m , purple) dipole moments of the S₀-to-S₁ transition for (a) (S,P)-**1**, (b) (S,M)-**1** and (c) (S)-**2** calculated at the B3LYP/6-31G*/LanL2DZ level. Calculated values of transition dipole moments ($|\mu_e|$, $|\mu_m|$ and $\theta_{e,m}$) and g_{abs} are given under each structure.

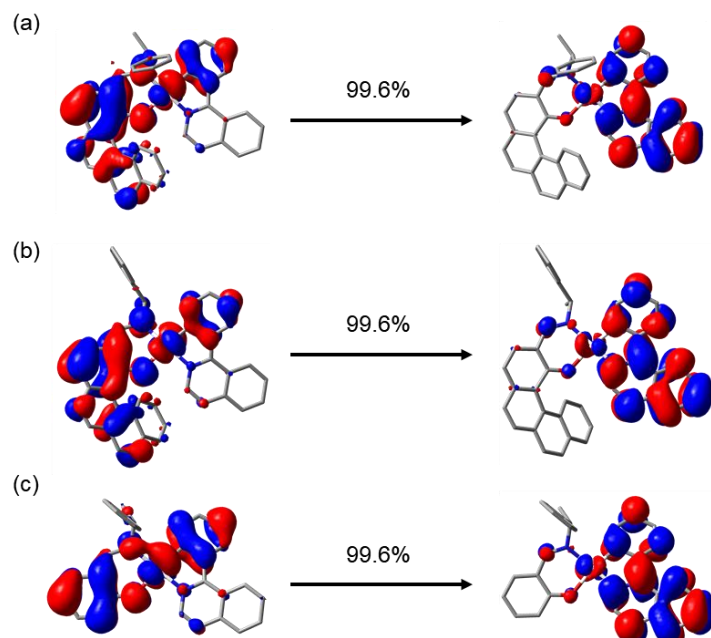


Fig. S23 NTO analysis of the S₀→S₁ transition for (a) (S,P)-**1**, (b) (S,M)-**1** and (c) (S)-**2** as obtained from DFT calculations (B3LYP/6-31G*, LanL2DZ).

7. Cartesian Coordinates (in Å)

Table S8. Cartesian coordinates (in angstrom) of (*S,P*)-**1** in the S₀ state^[a].

atom	x	y	z
Pt	-0.795838	-0.58009	-0.624634
O	1.29384	-0.253527	-0.319687
N	-1.192468	1.429436	-0.559063
N	-0.419979	-2.584421	-0.438832
C	-0.212488	2.340146	-0.302115
H	0.793908	1.941545	-0.302978
C	3.617913	-0.568249	-0.704071
C	5.183064	1.32876	-0.791551
C	-3.349776	0.698418	-1.117872
C	2.241084	-1.062619	-0.644937
C	-2.497131	1.777157	-0.600582
C	3.738886	2.831109	1.112799
C	0.755376	-3.091766	-0.708739
H	0.829678	-4.179886	-0.690305
C	-2.709021	-0.576062	-1.200219
C	4.776354	3.442925	0.343204
H	5.01468	4.488718	0.521619
C	4.027612	0.735608	-0.212062
C	-4.686577	-1.414202	-2.373115
H	-5.193453	-2.235495	-2.874768
C	6.043219	0.556118	-1.624934
H	6.937656	1.028303	-2.024573
C	5.512176	2.695508	-0.524934
H	6.365175	3.126732	-1.043632
C	4.555406	-1.347187	-1.445493
C	3.396852	1.458449	0.886023
C	-0.499873	3.656146	-0.061916
H	0.305704	4.362236	0.110512
C	-1.852671	4.06824	0.036958
C	2.541915	0.840828	1.836172
H	2.344254	-0.218841	1.764022
C	-4.228253	3.479608	0.084523
H	-5.013739	2.737089	0.044168
C	-2.884656	3.097797	-0.186502
C	-2.206318	5.394741	0.398088
H	-1.412305	6.12296	0.541359
C	-4.62377	0.892188	-1.684271
H	-5.070388	1.878443	-1.71581
C	-1.367463	-3.390184	1.711056
C	-3.404225	-1.604905	-1.854282
H	-2.925881	-2.568412	-2.003828
C	-2.480965	-2.963634	2.444185

H	-3.378196	-2.649112	1.916492
C	1.994713	-2.434667	-0.984167
C	-4.53855	4.768179	0.462426
H	-5.570118	5.032018	0.67736
C	-5.300451	-0.16321	-2.288738
H	-6.281763	0.001143	-2.724905
C	-3.523261	5.743859	0.592841
H	-3.783256	6.759571	0.87785
C	-1.451182	-3.46074	0.18602
H	-2.405953	-3.021895	-0.093862
C	3.041422	-3.231476	-1.532511
H	2.828402	-4.270207	-1.777533
C	5.783271	-0.760568	-1.870047
H	6.475211	-1.366608	-2.449289
C	4.263292	-2.694394	-1.814278
H	5.030306	-3.276453	-2.316931
C	1.972927	1.554242	2.873109
H	1.328928	1.042899	3.583282
C	-1.452149	-4.91608	-0.314819
H	-1.461415	-4.956415	-1.410225
H	-2.357412	-5.408008	0.055012
H	-0.601801	-5.499643	0.051882
C	3.108843	3.552556	2.15845
H	3.368659	4.600386	2.292998
C	-2.449046	-2.929594	3.840062
H	-3.323402	-2.593504	4.391263
C	2.228481	2.93303	3.020543
H	1.764202	3.491892	3.828839
C	-0.213666	-3.775602	2.406625
H	0.670009	-4.096132	1.860452
C	-0.176532	-3.739635	3.800463
H	0.728156	-4.039109	4.323127
C	-1.296072	-3.318268	4.522619
H	-1.266353	-3.289452	5.608571

[a] The geometry was optimized by DFT calculation (B3LYP/6-31G*, LanL2DZ).

Table S9. Cartesian coordinates (in angstrom) of (*S,M*)-**1** in the S_0 state^[a].

atom	x	y	z
Pt	0.69798	0.514764	-0.100048
O	-0.632777	-1.155331	-0.011542
N	-0.876945	1.791035	-0.416897
N	2.207957	-0.758474	0.446607
C	-2.161837	1.341621	-0.473538
H	-2.268832	0.265187	-0.494212
C	-1.402314	-3.378821	-0.358503
C	-3.741531	-3.863913	-0.9487
C	0.846979	3.370599	-0.586709
C	-0.334165	-2.401142	-0.144759
C	-0.584655	3.109236	-0.396152
C	-4.75424	-1.727038	0.59324
C	2.11563	-2.05735	0.303845
H	3.00998	-2.62457	0.572032
C	1.686144	2.21874	-0.472145
C	-5.597312	-2.41391	-0.334384
H	-6.639939	-2.116265	-0.415675
C	-2.815119	-3.077836	-0.209791
C	3.560175	3.61133	-1.211337
H	4.615173	3.691522	-1.463191
C	-3.310516	-5.059501	-1.594103
H	-4.048842	-5.657053	-2.123685
C	-5.11911	-3.484921	-1.025971
H	-5.777124	-4.074751	-1.659781
C	-1.025364	-4.641052	-0.905955
C	-3.372737	-2.089502	0.705209
C	-3.224563	2.203101	-0.497248
H	-4.234056	1.812858	-0.572287
C	-2.999506	3.593571	-0.338623
C	-2.649899	-1.549548	1.801057
H	-1.637113	-1.879463	1.982486
C	-1.442081	5.429526	0.102728
H	-0.441846	5.783746	0.312671
C	-1.648561	4.062025	-0.231849
C	-4.071154	4.518411	-0.232333
H	-5.087891	4.149387	-0.338862
C	1.372288	4.595257	-1.040211
H	0.719919	5.438823	-1.229218
C	3.0388	2.379824	-0.807973
H	3.709337	1.527951	-0.794102
C	1.020456	-2.867011	-0.122674
C	-2.504507	6.298327	0.229696

H	-2.322517	7.334461	0.500313
C	2.726686	4.723719	-1.331789
H	3.118449	5.673856	-1.683895
C	-3.830104	5.847499	0.031578
H	-4.657488	6.546099	0.120542
C	3.381954	-0.269155	1.23478
H	3.417401	0.805352	1.056033
C	1.316244	-4.216914	-0.473875
H	2.353264	-4.544619	-0.44345
C	-2.015598	-5.478456	-1.498177
H	-1.703534	-6.426595	-1.92853
C	0.338639	-5.060198	-0.914124
H	0.576692	-6.057316	-1.27309
C	-3.217463	-0.632731	2.664271
H	-2.634635	-0.250101	3.497742
C	-5.301043	-0.751195	1.464813
H	-6.346868	-0.477353	1.343136
C	-4.546497	-0.199826	2.479054
H	-4.981461	0.533921	3.152512
C	4.713139	-0.860521	0.759801
C	4.999946	-0.916617	-0.615803
C	5.696935	-1.299009	1.655494
C	6.228599	-1.38654	-1.076371
H	4.244262	-0.606711	-1.33202
C	6.93046	-1.770405	1.195857
H	5.511184	-1.27551	2.724073
C	7.202425	-1.81477	-0.17039
H	6.424038	-1.420894	-2.144951
H	7.676189	-2.10513	1.912252
H	8.160551	-2.182232	-0.527826
C	3.08505	-0.455125	2.729995
H	2.103481	-0.027627	2.954009
H	3.072317	-1.514358	3.011796
H	3.828556	0.061848	3.345714

[a] The geometry was optimized by DFT calculation (B3LYP/6-31G*, LanL2DZ).

Table S10. Cartesian coordinates (in angstrom) of (*S*)-**2** in the S₀ state^[a].

atom	x	y	z
Pt	0.008713	0.26089	-0.473148
O	0.67565	2.221641	-0.007054
C	-1.001388	-1.358131	-1.101153
C	3.008952	1.900858	-0.51009
C	1.858833	2.707104	-0.215365
C	3.044934	-2.083058	0.894229
N	-1.915333	0.8453	-0.063022
C	-4.433653	1.431019	0.977823
C	-2.40038	-1.324615	-0.803718
C	2.979634	0.472772	-0.552501
H	3.970421	0.014112	-0.542957
C	4.273252	2.526665	-0.682232
H	5.135793	1.894987	-0.88676
C	-4.114099	0.096203	0.564556
C	-5.039826	-0.937647	0.877352
H	-4.772527	-1.969112	0.691028
N	1.969665	-0.357563	-0.56359
C	-6.248522	-0.651949	1.475549
H	-6.932919	-1.459881	1.717802
C	-0.560418	-2.388828	-1.945438
H	0.476419	-2.425874	-2.256754
C	2.315091	-1.900456	2.08064
H	1.284072	-1.560442	2.020415
C	2.898552	-2.137598	3.322927
H	2.316556	-1.98881	4.228676
C	-2.846393	-0.132355	-0.075388
C	3.111742	-2.286353	-1.680886
H	3.265547	-3.369913	-1.638838
H	2.542607	-2.051855	-2.58525
H	4.092689	-1.810738	-1.781634
C	2.05436	4.116797	-0.119285
H	1.183485	4.724024	0.109175
C	-3.44615	2.439033	0.834141
H	-3.657868	3.459493	1.137572
C	4.371477	-2.518837	0.988748
H	4.959808	-2.683814	0.091301
C	4.426905	3.893705	-0.602896
H	5.39989	4.352447	-0.748282
C	-2.20196	2.103629	0.375309
H	-1.370333	2.795981	0.327486
C	4.958644	-2.760185	2.235305
H	5.99	-3.099685	2.285844

C	-5.698035	1.698643	1.563749
H	-5.932798	2.720591	1.849872
C	-2.791723	-3.306082	-2.160082
H	-3.477822	-4.034057	-2.583683
C	-1.428304	-3.358471	-2.452206
H	-1.041686	-4.137621	-3.105297
C	2.3469	-1.809476	-0.43962
H	1.397624	-2.340451	-0.407857
C	3.294176	4.688002	-0.316287
H	3.401356	5.768069	-0.244021
C	-3.275525	-2.278858	-1.356672
H	-4.346015	-2.190648	-1.217478
C	-6.595529	0.680759	1.795172
H	-7.557392	0.893871	2.25324
C	4.226126	-2.569093	3.405152
H	4.68196	-2.756538	4.373694

[a] The geometry was optimized by DFT calculation (B3LYP/6-31G*, LanL2DZ).

Table S11. Cartesian coordinates (in angstrom) of (*S,P*)-**1** in the T₁ state^[a].

atom	x	y	z
Pt	-0.842408	-0.613567	-0.550524
O	1.232995	-0.292773	-0.173851
N	-1.27461	1.399191	-0.430438
N	-0.428201	-2.58669	-0.460469
C	-0.320349	2.313818	-0.103441
H	0.690858	1.929056	-0.063762
C	3.491243	-0.364659	-0.908365
C	4.94012	1.626804	-1.021383
C	-3.399324	0.64295	-1.085255
C	2.190404	-0.962527	-0.734578
C	-2.579757	1.73022	-0.523892
C	3.647486	2.884442	1.166352
C	0.742125	-3.061868	-0.951
H	0.78261	-4.125184	-1.178971
C	-2.745599	-0.624421	-1.149449
C	4.537808	3.620244	0.321651
H	4.729878	4.66608	0.55049
C	3.892956	0.916015	-0.350084
C	-4.701071	-1.510823	-2.314869
H	-5.200099	-2.348763	-2.796112
C	5.742503	0.989426	-2.001124
H	6.551466	1.548904	-2.46249
C	5.202126	2.995685	-0.688322
H	5.949448	3.527785	-1.272062
C	4.411621	-1.020075	-1.798304
C	3.363638	1.51046	0.870732
C	-0.635952	3.620702	0.152864
H	0.151226	4.332257	0.379723
C	-1.996728	4.013719	0.193223
C	2.669404	0.772215	1.86535
H	2.51817	-0.289136	1.73131
C	-4.36484	3.397832	0.111899
H	-5.139076	2.648575	0.01922
C	-3.004842	3.035862	-0.101461
C	-2.383576	5.328344	0.564566
H	-1.606186	6.061651	0.762269
C	-4.662291	0.814721	-1.679455
H	-5.119654	1.794875	-1.735263
C	-1.019257	-3.516825	1.75143
C	-3.423675	-1.679992	-1.774711
H	-2.937627	-2.645529	-1.875079
C	-1.985509	-3.090732	2.670574

H	-2.947771	-2.736932	2.307627
C	1.930091	-2.344578	-1.199487
C	-4.708056	4.67419	0.501179
H	-5.751871	4.921779	0.671605
C	-5.318335	-0.259972	-2.276107
H	-6.292561	-0.111336	-2.73334
C	-3.712235	5.658523	0.701582
H	-3.998348	6.664754	0.994897
C	-1.338105	-3.508189	0.25511
H	-2.334278	-3.076868	0.148454
C	2.974031	-3.006079	-1.897586
H	2.811996	-4.027743	-2.232588
C	5.531099	-0.336429	-2.3107
H	6.190136	-0.856124	-3.002312
C	4.140758	-2.357157	-2.219807
H	4.887279	-2.862368	-2.828807
C	2.197825	1.369901	3.019307
H	1.677435	0.765159	3.757067
C	-1.395366	-4.935154	-0.321406
H	-1.584278	-4.91727	-1.401069
H	-2.215731	-5.474854	0.162689
H	-0.480442	-5.505871	-0.135858
C	3.11828	3.484033	2.334363
H	3.333002	4.534566	2.519043
C	-1.72726	-3.1114	4.04305
H	-2.491146	-2.77773	4.74068
C	2.390976	2.746484	3.247709
H	2.001269	3.213245	4.148383
C	0.220611	-3.957201	2.236411
H	0.991158	-4.275554	1.53935
C	0.483431	-3.974408	3.605965
H	1.451038	-4.316264	3.964414
C	-0.491186	-3.553989	4.51517
H	-0.285717	-3.568908	5.582279

[a] The geometry was optimized by DFT calculation (B3LYP/6-31G*, LanL2DZ).

Table S12. Cartesian coordinates (in angstrom) of (*S,M*)-**1** in the T₁ state^[a].

atom	x	y	z
Pt	0.72862	0.470126	-0.029815
O	-0.639851	-1.157742	0.210905
N	-0.822573	1.79257	-0.32898
N	2.197086	-0.836688	0.466643
C	-2.122853	1.389756	-0.283267
H	-2.270205	0.319731	-0.220934
C	-1.540789	-3.254003	-0.460814
C	-3.896657	-3.577673	-1.114383
C	0.950929	3.289608	-0.675056
C	-0.435581	-2.387029	-0.142953
C	-0.483759	3.09626	-0.414993
C	-4.825665	-1.57381	0.665555
C	2.089865	-2.157766	0.197332
H	3.005081	-2.738055	0.302351
C	1.75624	2.122109	-0.504249
C	-5.681685	-2.102659	-0.352403
H	-6.70584	-1.741435	-0.412929
C	-2.942188	-2.917447	-0.272468
C	3.673119	3.409755	-1.308427
H	4.732216	3.447165	-1.552246
C	-3.531071	-4.710955	-1.881447
H	-4.288794	-5.207352	-2.481049
C	-5.249076	-3.105557	-1.163907
H	-5.926304	-3.574253	-1.873864
C	-1.242832	-4.496581	-1.124926
C	-3.464648	-2.018036	0.746388
C	-3.155214	2.287681	-0.312089
H	-4.179984	1.931331	-0.304793
C	-2.873364	3.675507	-0.26875
C	-2.734894	-1.638691	1.903845
H	-1.738359	-2.02909	2.053164
C	-1.232931	5.47885	-0.045718
H	-0.212294	5.810572	0.08743
C	-1.502285	4.098582	-0.266899
C	-3.906014	4.645351	-0.176543
H	-4.938726	4.307719	-0.202515
C	1.51053	4.463483	-1.210273
H	0.88476	5.314232	-1.449795
C	3.115656	2.22092	-0.829252
H	3.76078	1.355116	-0.738546
C	0.955701	-2.889295	-0.206839
C	-2.257155	6.393227	0.070294

H	-2.026016	7.438572	0.253952
C	2.868636	4.530326	-1.51217
H	3.286306	5.443203	-1.927474
C	-3.606442	5.979831	-0.025629
H	-4.403503	6.71391	0.053282
C	3.350552	-0.428751	1.303018
H	3.402859	0.659225	1.216162
C	1.151224	-4.219412	-0.657962
H	2.161667	-4.619752	-0.682118
C	-2.246219	-5.209038	-1.806209
H	-1.977579	-6.128516	-2.32112
C	0.104742	-4.969121	-1.140162
H	0.297619	-5.952283	-1.563942
C	-3.274818	-0.801905	2.863042
H	-2.685434	-0.545022	3.739265
C	-5.341571	-0.684388	1.637899
H	-6.372006	-0.349647	1.537762
C	-4.578863	-0.289144	2.719847
H	-4.990074	0.381922	3.469099
C	4.694436	-0.986538	0.811403
C	4.97407	-1.039923	-0.565507
C	5.699823	-1.390211	1.700291
C	6.214971	-1.470121	-1.033784
H	4.202368	-0.760886	-1.276747
C	6.945219	-1.820601	1.23365
H	5.521698	-1.371984	2.770136
C	7.20976	-1.860809	-0.13449
H	6.40225	-1.503788	-2.103973
H	7.706692	-2.127182	1.946207
H	8.177287	-2.197036	-0.497474
C	3.03063	-0.739656	2.776614
H	2.046413	-0.329436	3.020203
H	3.011047	-1.819179	2.962083
H	3.763772	-0.279647	3.447482

[a] The geometry was optimized by DFT calculation (B3LYP/6-31G*, LanL2DZ).

Table S13. Cartesian coordinates (in angstrom) of (*S*)-**2** in the T₁ state^[a].

atom	x	y	z
Pt	0.010665	0.257425	-0.424506
O	0.673469	2.193376	0.1304
C	-0.979267	-1.320442	-1.124913
C	2.982313	1.935894	-0.518822
C	1.835467	2.708323	-0.135938
C	3.09936	-2.069706	0.849029
N	-1.880275	0.842488	-0.011793
C	-4.517949	1.38993	0.876655
C	-2.404242	-1.31636	-0.788087
C	2.984125	0.504499	-0.585441
H	3.985063	0.068625	-0.611339
C	4.219625	2.592044	-0.746597
H	5.081818	1.985226	-1.01703
C	-4.148432	0.034046	0.577602
C	-5.046551	-0.979779	0.942842
H	-4.75938	-2.018686	0.836892
N	1.992064	-0.342324	-0.57856
C	-6.306823	-0.677135	1.488099
H	-6.980499	-1.490401	1.744069
C	-0.524168	-2.329856	-1.985767
H	0.50661	-2.324575	-2.318662
C	2.36196	-1.951031	2.038658
H	1.315718	-1.659547	1.98672
C	2.956422	-2.190266	3.275441
H	2.368176	-2.091617	4.183918
C	-2.860905	-0.199651	-0.051214
C	3.15603	-2.243207	-1.728055
H	3.328855	-3.324073	-1.694285
H	2.577883	-2.012824	-2.627789
H	4.128174	-1.750833	-1.831947
C	2.008361	4.116807	-0.009605
H	1.141571	4.698096	0.290362
C	-3.541857	2.414465	0.665874
H	-3.781268	3.448603	0.891104
C	4.445278	-2.444096	0.933734
H	5.04045	-2.559896	0.033056
C	4.350596	3.961619	-0.640077
H	5.30401	4.444164	-0.830565
C	-2.234339	2.081663	0.291886
H	-1.436244	2.815569	0.260031
C	5.043484	-2.687599	2.174434
H	6.089615	-2.979447	2.21765

C	-5.783303	1.670249	1.415444
H	-6.048852	2.705378	1.615711
C	-2.728075	-3.344142	-2.105307
H	-3.38598	-4.113838	-2.500572
C	-1.362432	-3.337007	-2.460493
H	-0.970309	-4.105361	-3.121544
C	2.390843	-1.790978	-0.477755
H	1.448559	-2.335297	-0.449082
C	3.223251	4.721859	-0.26431
H	3.311847	5.801565	-0.167312
C	-3.244074	-2.35328	-1.297871
H	-4.310446	-2.324175	-1.111311
C	-6.687603	0.641634	1.707736
H	-7.665025	0.874556	2.119567
C	4.302924	-2.560014	3.347998
H	4.767415	-2.749426	4.311993

[a] The geometry was optimized by DFT calculation (B3LYP/6-31G*, LanL2DZ).

8. References

- S1. E. Yen-Pon, F. Buttard, L. Frédéric, P. Thuéry, F. Taran, G. Pieters, P. A. Champagne and D. Audisio, *JACS Au*, 2021, **1**, 807.
- S2. D. Kourkoulos, C. Karakus, D. Hertel, R. Alle, S. Schmeding, J. Hummel, N. Risch, E. Holder and K. Meerholz, *Dalton Trans.*, 2013 **42**, 13612.
- S3. P. A. A. M. Vaz, J. Rocha, A. M. S. Silva and S. Guieu, *New J. Chem.*, 2018, **42**, 18166.
- S4. Gaussian 16, Revision C.01, M. J. Frisch, G. W. Trucks, H. B. Schlegel, G. E. Scuseria, M. A. Robb, J. R. Cheeseman, G. Scalmani, V. Barone, G. A. Petersson, H. Nakatsuji, X. Li, M. Caricato, A. V. Marenich, J. Bloino, B. G. Janesko, R. Gomperts, B. Mennucci, H. P. Hratchian, J. V. Ortiz, A. F. Izmaylov, J. L. Sonnenberg, D. Williams-Young, F. Ding, F. Lipparini, F. Egidi, J. Goings, B. Peng, A. Petrone, T. Henderson, D. Ranasinghe, V. G. Zakrzewski, J. Gao, N. Rega, G. Zheng, W. Liang, M. Hada, M. Ehara, K. Toyota, R. Fukuda, J. Hasegawa, M. Ishida, T. Nakajima, Y. Honda, O. Kitao, H. Nakai, T. Vreven, K. Throssell, J. A. Montgomery, Jr., J. E. Peralta, F. Ogliaro, M. J. Bearpark, J. J. Heyd, E. N. Brothers, K. N. Kudin, V. N. Staroverov, T. A. Keith, R. Kobayashi, J. Normand, K. Raghavachari, A. P. Rendell, J. C. Burant, S. S. Iyengar, J. Tomasi, M. Cossi, J. M. Millam, M. Klene, C. Adamo, R. Cammi, J. W. Ochterski, R. L. Martin, K. Morokuma, O. Farkas, J. B. Foresman and D. J. Fox, Gaussian, Inc., Wallingford CT, 2016.